Modeling Earth Systems and Environment (2021) 7:1475–1502
https://doi.org/10.1007/s40808-020-00866-y

ORIGINAL ARTICLE

Predictive model and assessment of the potential for wind and solar power in Rayak region, Lebanon

Youssef Kassem[1,2] · Hüseyin Gökçekuş[2] · Wassim Janbein[2]

Received: 15 April 2020 / Accepted: 24 June 2020 / Published online: 3 July 2020

Abstract

With the increasing consumption of fossil fuel, reducing greenhouse gas (GHG) emissions has become a serious issue that has attracted worldwide attention. Therefore, Lebanon is currently interested in utilizing renewable energy technologies to reduce energy dependence on oil reserves and GHG emissions. The present study is focused on solar and wind power potential and the economic viability of wind/solar systems for the Rayak region in Lebanon for the first time. The input data sources for the study including the Meteorological data for wind speed and NASA database for solar energy. In the assessment of wind energy, a two-parameter Weibull distribution function was used to analyze the characteristics of wind speed. Yearly and seasonal Weibull parameters were calculated for 10 m height using the Maximum likelihood method. In addition, yearly and seasonal wind power density values were calculated. The results showed that the mean annual wind speed and wind power density values were 5.884 m/s and 124.534 W/m^2, respectively, during the investigation period. It can be concluded that the value of wind power density at the region was classified as marginal wind power potential and high-scale wind turbines can be used to gather wind energy potential in the region. Furthermore, predicting wind speed depends on various atmospheric factors and random variables. Therefore, 63 ANN models are developed by varying the meteorological parameters to predict the daily wind speed in the selected region. All the models with various combinations are validated and the performances of the models are analyzed using root mean squared error. The results demonstrated that the most relevant input variables for predicting the daily wind speed were found to be temperature, pressure, and relative humidity. In the assessment of wind energy, average monthly global solar radiation data were evaluated. It is found that the annual global solar radiation was 1877.41 kWh/m^2, which indicates the selected region has high solar resources and is categorized as an excellent potential class. Moreover, this study provides a comprehensive and integrated feasibility analysis of 100 MW grid-connected wind and solar projects economic projects that can be developed in the country to reduce the electricity crisis and GHG emissions. Several different economic and financial indicators were calculated. The results indicate that the wind farm is a more economical option than the solar plant because of the higher values of NPV, BCR, ALCS, and IRR as well as the lower values of EB, SB, and LCOE.

Keywords ANN · Techno-economic · Lebanon · Rayak region · Retscreen expert software · Wind potential · Solar potential

✉ Youssef Kassem
youssef.kassem@neu.edu.tr;
youssef.kassem1986@hotmail.com

Hüseyin Gökçekuş
huseyin.gokcekus@neu.edu.tr

Wassim Janbein
wassimjanbein@gmail.com

[1] Department of Mechanical Engineering, Engineering Faculty, Near East University, (via Mersin 10, Turkey), 99138 Nicosia, Cyprus

[2] Department of Civil Engineering, Civil and Environmental Engineering Faculty, Near East University, (via Mersin 10, Turkey), 99138 Nicosia, Cyprus

Introduction

The utilization of solar and wind energy is expected to increase more than any other energy source by the middle of this century (Owusu and Asumadu-Sarkodie 2016; Osinowo et al. 2017). Solar and wind energy are clean and renewable sources of energy (Prasad et al. 2017; Kassem 2018). Therefore, wind and solar energy are alternative energy sources and are being progressively adapted in numerous applications(Zendehboudi et al. 2018; Chang and Starcherl 2019). Many studies have been investigated by solar and wind energy generated electricity potential in

many countries worldwide to generate power. For example, Zhou et al. (2011) evaluated the onshore wind energy potential in Juangsu province, china based on meteorological data from 1979 to 2008. The results indicated that the annual power production from wind found to be 146,336 GWh in the selected location. Ahmed (2019) presented the technical assessment of a two wind farm of 300 MW-installed capacity at chosen regions in Egypt. It is found that the annual power production from the proposed wind farms is found to be 1130 GWh and the expected cost was varied from 1.96€ to 2.09 € cents/kWh. Dabar et al. (2019) assessed the wind potential in the Republic of Djibouti based on 3 years by meteorological stations at eight locations. In addition, they examined the feasibility of three wind farms of 275 MW installed capacity at GaliMa-aba, Ghoubbet, and Bada Wein. The results showed that the proposed wind farms would produce 1073 GWh/year of electricity and the expected cost was varied from 7.03 to 9.67 US.$ cent/kWh. Chadee et al. (2018) conducted the technical and economic assessments to estimate the expected cost of electricity generation from wind in Trinidad and Tobago islands based on long-term measurements of wind speed. The results found that electricity cost for the large wind turbines, 1500 kW and greater, were less than the current subsidized residential tariff of the US/$0.06/kWh. Parikh et al. (2019) determined the variation in electricity solar potential by utilizing different types of solar panels. The results concluded that the maximum value of power generated from the proposed farm was estimated to be 173.6 MW. Rehman et al. (2017) presented the feasibility of 10 MW grid-connected PV plants at 44 sites in Saudi Arabia. It is found that the best location for the future installation of a PV plant was found to be Bisha due to the highest solar radiation intensity and longer sunshine duration. Adaramola (2014) studied the feasibility of the PV grid-tied energy system in Jos, Nigeria using HOMER software. The results showed that the system could be produced energy of 331.536 GWh/year with a capacity factor of 40.4% from solar energy.

Lebanon, which is located in the Eastern Mediterranean, covers a total area of 10,452 km^2, with a coastline of about 220 km from north to south. Lebanon borders Syria to the north and east, and Israel to the south. Geographically, Lebanon consists of a narrow coastal strip that extends parallel to the Mediterranean Sea and two mountain ranges, namely Mount Lebanon and the East Lebanon Mountain Range or Qalamoun Mountains, running from north to south. The fertile Bekaa Valley is located between the two ranges. Lebanon usually has a Mediterranean climate, with cold and rainy winters from the month of December until mid-March, and hot and dry summers that begin in June and ends in September. Average temperatures across the country vary from 20 °C on the coast to 17 °C in the Bekaa Valley and less than 10 °C in the mountains.

Electricity of Lebanon

Lebanon is among the few countries in the world without electricity 24/7, and suffers from a large energy deficit. The energy production depends on fuel oil, diesel oil, and other imports, in which results in electricity blackout periods that range from 4 to 14 h in all Lebanese regions and sometimes more. Currently, the electrical energy in Lebanon is generated by oil products, hydropower, and importation. The power plants in Lebanon are classified as thermal and hydroelectric. In fact, Lebanon has 13 power plants with a total capacity of 3016 MW distributed as 2764 MW thermal plants and 252.6 MW hydropower plants. Statistics indicate that 97% of the total energy was generated by thermal plants in 2015 and hydropower had a share of only 2.6% in that year, as shown in Fig. 1. The electricity crisis is one of the most significant issues affecting the daily lives of citizens, shop owners, and small businesses which has been at

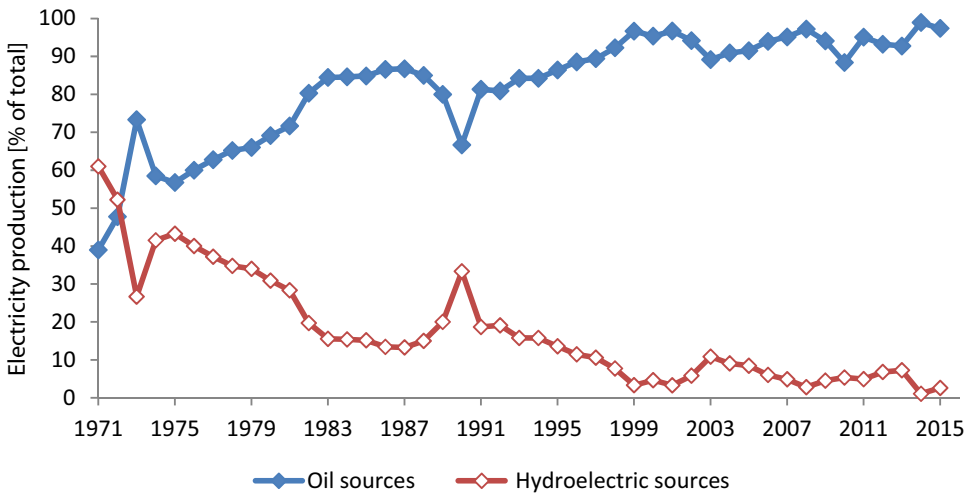

Fig. 1 Electricity production from oil and hydroelectrically sources (World Bank 2019)

the forefront of daily life in Lebanon for years. Lebanon is experiencing a real crisis because of the power cuts that have continued for many years without any proven solutions. The electricity service is becoming worse in Lebanon. According to the Lebanon News, the number of hours during which the electricity supply is disrupted in all cities of the country is increasing day by day. Lebanon is not a country isolated from the world and the electricity sector crisis cannot be separated from the conditions of the global economy. International oil prices play a major role in increasing the deficit in the EDL. The higher the price of oil globally, the more the EDL losses will increase, because 85% of the country's energy production is dependent on this oil. In addition, the causes of the crisis in the electrical sector in Lebanon are the lack of alternatives to petroleum and the low production capacity (the Electricity Corporation produces 1500 mW, while the demand reaches three thousand megawatts, which requires the construction of new factories). Therefore, the increase in the population and subsequent demand for energy have enhanced the significance of renewable energy as an alternative source in recent years.

Currently, special diesel generators (DG) distributed throughout the country are used to meet the energy consumption needs of the population. During periods of power outages, the central public directorates in each region take responsibility and provide users with electrical energy. Subscriptions vary according to the needs of each consumer. While the majority of apartments may settle for the cheapest offer, general managers provide 1.1 kVA, and other citizens residing in larger homes with a higher standard of living tend to subscribe to more expensive offers that provide 2.2–4.4 kVA. The resulting fees increase in accordance with the subscription. It is worth noting that most of the time. On the other hand, industries, hospitals, offices, and centers tend to install their own generators according to their energy consumption. This solution provides them with complete control over electricity production during a power outage and helps reduce the fees generated, or at least the ability to manage them. Installing DGs is an alternative solution that not only causes massive air pollution, but is very uncomfortable due to the industry's medium regulation. Moreover, it does not provide flexibility to the user, meaning that a fixed amount of money is imposed on the population independently of the amount of energy consumed. The resulting fees are highly influenced by fuel prices and blackout hours. Recently, Lebanese municipalities began charging a fixed monthly tariff for each subscription to try to contain the chaos and price differentials between different regions of the country.

Renewable energy in Lebanon

Lebanon is located in the Eastern Mediterranean with a surface area of 10,452 km^2 and a coastline of 220 km. The population in the country is estimated to be 4 million. As the Lebanese electricity system is mainly based on thermal energy, large volumes of dangerous gases are emitted into the atmosphere on a daily basis. According to Chedid et al. (2001), the energy sector in Lebanon was found to contribute 85% of all CO_2 emissions and 96% of all SO_2 emissions. Therefore, renewable energy projects account for a worldwide decrease in CO_2 levels in several countries. Renewable energies are offered by natural sources that can be persistently and sustainably replenished. In general, PV, wind and hydropower are the most interesting resources to explore in Lebanon. As mentioned previously, around 2% of the total energy in the country is produced by hydropower stations. According to the UNDP, the wind potential is estimated to be 1500 MW in Lebanon. Moreover, according to Abdeladim et al. (2018), Lebanon has high levels of sunshine hours and the daily average solar insolation is about 4.8 kWh/m^2. Numerous studies have investigated the potential of renewable energy in terms of solar energy and wind energy in Lebanon. For instance, Al Zohbi et al. (2015) investigated the characteristics of wind speed for five locations in Lebanon. They found that wind power could reduce the electricity demand in Lebanon. Zohbi et al. (2016) evaluated the performance of a hybrid wind-hydro power plant in two dams in Lebanon to find the best dam to generate energy by wind power at night. The authors concluded that a combination of wind energy with a pumped hydro storage system could be an ideal solution to solve Lebanon's electricity crisis. Kassem et al. (2019a, b, c, d, e) investigated the wind potential in three coastal regions (Beirut, Sidon, and Tripoli) in Lebanon. The authors found that vertical axis wind turbines have the potential to outperform horizontal axis wind turbines in urban environments. Gökçekuş et al. (2019) analyzed the wind speed characteristics and wind energy potential at eight selected locations in Northern Lebanon. They concluded that small-scale wind turbine use could be suitable for generating electricity in the studied regions. Kassem et al. (2019a, b, c, d, e) investigated the wind potential at certain selected regions in Lebanon using the Two-Parameter Weibull distribution function. The results indicated that the wind speeds at the selected regions were within the range of 2.627 m/s and 3.56 m/s. Furthermore, the wind speed densities varied between 14.634 and 25.280 W/m^2, which is classified as poor wind power. Tannous et al. (2018) investigated and compared traditional grid-connected and solar stand-alone systems for two street lighting technologies in Lebanon. The results showed that the solar system had a lesser overall environmental impact than the traditional system. Ibarra-Berastegi et al. (2019) evaluated the Lebanese offshore-wind-energy potential. They found that wind power density along the shore of the northern coastal area exhibited the highest potential and reached r values of around 400 W/m^2 in the winter. Elkhoury et al. (2010) investigated the

feasibility of wind turbine farms for generating electricity in four sites in Lebanon. The results indicated that Zahleh and Beirut have high wind energy potential. Nakad et al. (2012) studied the techno-economic feasibility of a wind farm in the Zahleh region taking into consideration the land area and the appropriate turbines.

Importance of the study

Based on the literature review, it is evident that there is a clear lack of utilization of wind energy potential as power generation sources in Lebanon. To the best of the author's knowledge, no study has investigated the wind potential in the city of Rayak, Lebanon. Moreover, no study has focused on the feasibility of a 100 MW grid-connected wind/PV in the selected city to find the most economic project in the region. According to electricity of Lebanon (Électricité du Liban), the total power for Beqaa Valley is estimated to be 300 MWh. This study aims to reduce the electricity consumption generated by diesel fuel by 33%. Therefore, the aim of this paper is to analyze the wind speed characteristics for Rayak city, Bekaa, Lebanon based on data measured at height of 10 m Meteorology department. The hourly data cover the period of 1996–2006. In addition, to identify the meteorological parameters that influenced the prediction of wind speed, 63 ANN models were developed. Moreover, the monthly NASA database is used to assess the solar potential in the selected region. Furthermore, the use of wind or solar energy to power such systems may solve the electricity crises in the country and reduce GHG emissions. In this regard, the feasibility of a 100 MW grid-connected wind/PV project is presented. For this purpose, RETScreen Expert software is used.

Materials and methods

In this section, the potential of wind and solar energy is discussed. To investigate the wind potential, the wind speed characteristics, which were measured at a height of 10 m at Rayak region, are statistically analyzed. The Weibull distribution function is used to determine the wind power density in the selected locations. Furthermore, the power-law method is utilized to estimate the wind speed at various hub heights. Moreover, in general, there are several variables that can influence the potential wind resource in a specific region. In addition, the prediction of wind speed is important for estimating the wind power density in the region; thus, determining the most significant parameters is an important task to achieve accurate predictions of wind speed. In this study, an Artificial Neural Network (ANN) is used to identify the most relevant parameters for the prediction of the daily wind speed of the selected region. Moreover, the solar energy potential in the chosen location is investigated based on NASA's average monthly global solar radiation data. In addition, for the future installation of a grid-connected 100 MW wind and solar system, RETScreen software is used to present technical, environmental, and economic aspects. Figure 2 illustrates the analysis procedure of the current study.

Location selection

Figure 3 shows a regional map of Lebanon. The location chosen for the present study is in the west of the country. Rayak is a city located in the Zahleh District, one of the districts of the Bekaa Governorate. The city of Rayak rises 930 m above sea level and extends over an area of 992 hectares (9.92 km^2). The city contains a military airport. In general, the Beqaa valley is named due to its location between the eastern and western chains, moving northeast to southwest, and creates a 30-km stretch over an area equal to one-third of Lebanon. Its average height is no more than 900 m, and its highest point is in Baalbek, and it is considered the area of water that divide the rivers of Orontes and Litani. In administrative terms, Beqaa Valley is divided into three sections: North Beqaa, Middle Beqaa and West Beqaa. In the Middle Beqaa region, the humidity is high in winter, with Riyak station recording 82% in January. In the summer, it is about 48%. The relative humidity trajectory is quite different in the coastal areas, as the data shows it that is at its highest in summertime and drops in the winter in the coastal areas. For example, the humidity in the Beirut area reaches its highest value in summer of approximately 73% in July and August and the lowest in November at 68%. In general, these areas do not experience an average of less than 68% in almost all months.

Wind data analysis procedure

Weibull probability density function

The Weibull distribution is the most commonly used for analyzing the wind speed (v) characteristics in a specific region. The maximum likelihood method (MLM) is widely used for estimating the Weibull parameters. The probability density ($f(v)$) and cumulative distribution ($F(v)$) functions for two-parameter Weibull distribution are expressed in Eqs. (1) and (2) (Khan et al. 2018; Alayat et al. 2018; Kassem et al. 2019c). In addition, the mean velocity of the two-parameter Weibull distribution ($\overline{v}$) can be calculated using Eq. (3):

$$f(v) = \left(\frac{k}{c}\right)\left(\frac{v}{c}\right)^{k-1} \mathrm{e}^{-\left(\frac{v}{c}\right)^{k}}, \tag{1}$$

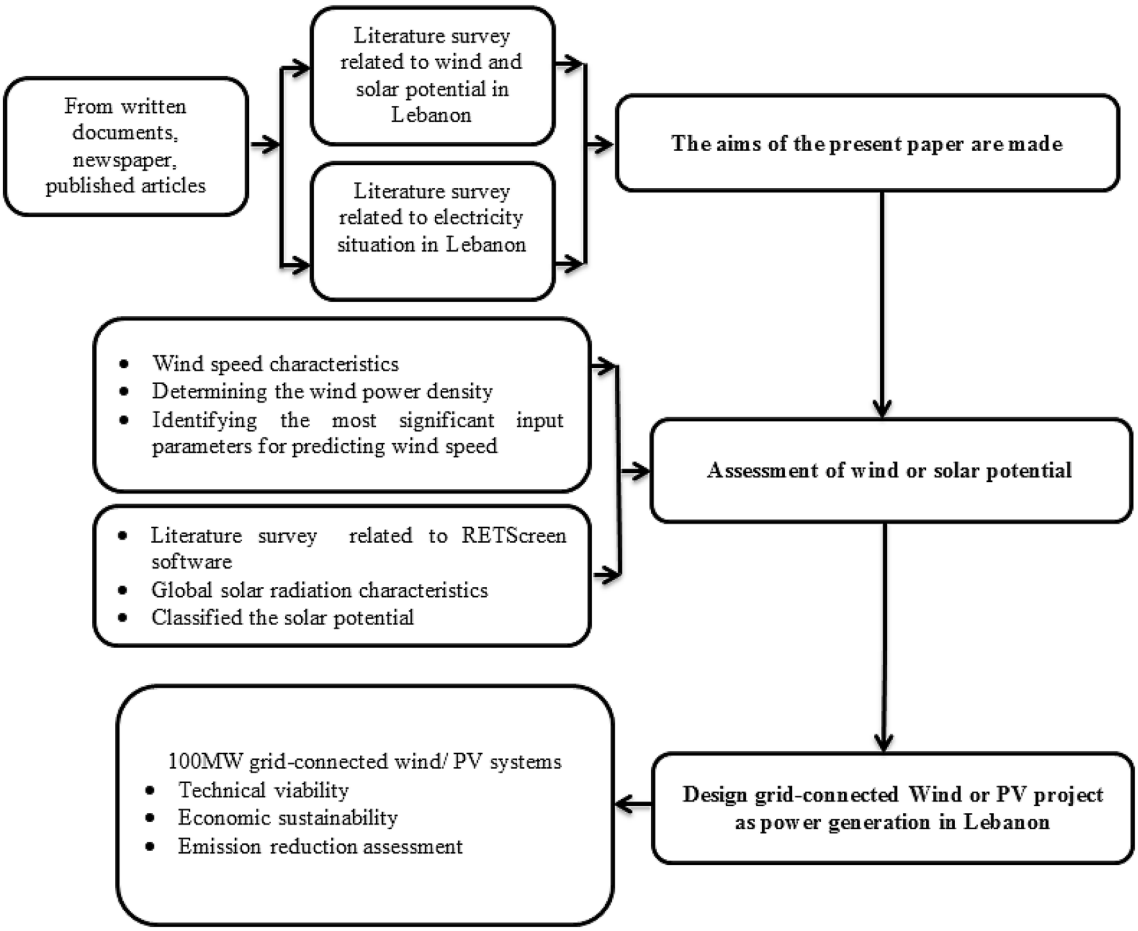

Fig. 2 Flowchart for analysis steps of the study

$$F(v) = 1 - \exp\left[-\left(\frac{v}{c}\right)^{k}\right], \tag{2}$$

$$\overline{v} = c\Gamma\left(1 + \frac{1}{k}\right), \tag{3}$$

where c is the scale parameter in m/s and k is the shape factor of distribution.

The Maximum likelihood method is a mathematical technique used to estimate the Weibull parameters through a numerical iteration. The Weibull parameter k and c values are calculated by the following equations (Kassem et al. 2019b, d):

$$k = \left(\frac{\sum_1^n v_i^k \ln\left(v_i\right)}{\sum_1^n v_i^k} - \frac{\sum_1^n \ln\left(v_i\right)}{n}\right)^{-1}, \tag{4}$$

$$c = \left(\frac{1}{n}\sum_1^n v_i^k\right)^{1/k}. \tag{5}$$

Moreover, the probable wind speed (V_{mp}) and maximum energy carrying wind speed (V_{maxE}) are essential wind speed indicators, which can be calculated using Weibull parameters as given below (Fazelpour et al. 2017; Pishgar-Komleh et al. 2015):

$$V_{mp} = c\left(1 - \frac{1}{k}\right)^{1/k}, \tag{6}$$

$$V_{maxE} = c\left(1 + \frac{2}{k}\right)^{1/k}. \tag{7}$$

Wind power density

The theoretically available kinetic energy that wind possesses at a certain location can be expressed as the mean wind power density (WPD). In other words, it is the maximum available wind power at each unit area. The mathematical expression for wind power density is given with

Fig. 3 Lebanon map

the following relations (Mohammadi et al. 2017; Kassem et al. 2019c):

$$\frac{P}{A} = \frac{1}{2}\rho v^3, \tag{8}$$

$$\frac{P}{A} = \frac{1}{2}\rho v^3 f(v). \tag{9}$$

Furthermore, WPD can be determined using Weibull parameters as follow (Keyhani et al. 2010):

$$\left(\frac{P}{A}\right)_W = \int_0^\infty \frac{1}{2}\rho v^3 f(v)\mathrm{d}v = \frac{1}{2}\rho c^3 \Gamma\left(1+\frac{3}{k}\right). \tag{10}$$

Moreover, the mean wind power density can be estimated using Eq. (11) (Irwanto et al. 2014):

$$\frac{\overline{P}}{A} = \frac{1}{2}\rho \overline{v}^3, \tag{11}$$

where P is the wind power density in W, $\overline{P}$ is the mean wind power density in W, A is the swept area in m^2, ρ is the air density, $f(v)$ is the probability density function (PDF), and $\overline{v}$ is the mean wind speed in m/s.

The monthly air density can be calculated using the following equations:

$$\rho = \frac{P_{\mathrm{av}}}{R_t \times T_{\mathrm{av}}}, \tag{12}$$

where P_{av} is the average air pressure in Pa, R_t is the specific gas constant (287 J/kg K) for air and T_{av} is the average air temperature in K.

In general, pressure, temperature and relative humidity are important factors affecting the air density, i.e., the air density is reduced by decreased air pressure, increased temperature and humidity (Danook et al. 2019).

The percentage errors in estimating the wind power density are calculated as follows:

$$\mathrm{Error} = \left|\frac{\left(\frac{P}{A}\right)_{\mathrm{W}} - \left(\frac{P}{A}\right)_{\mathrm{A}}}{\left(\frac{P}{A}\right)_{\mathrm{W}}}\right| \times 100\%, \tag{13}$$

where $\left(\frac{P}{A}\right)_{\mathrm{A}}$ is the actual wind power density and $\left(\frac{P}{A}\right)_{\mathrm{W}}$ is the Weibull wind power density.

Wind speed and air density extrapolation

The power law model is widely used to estimate the wind speed (v) at different wind turbine hub heights (z) (Gul et al. 2019; Shu et al. 2015). It is expressed as

$$\frac{v}{v_{10}} = \left(\frac{z}{z_{10}}\right)^{\alpha}, \tag{14}$$

where v_{10} is the wind speed at original height z_{10}, and α is the surface roughness coefficient (Eq. 14):

$$\alpha = \frac{0.37 - 0.088\ln\left(v_{10}\right)}{1 - 0.088\ln\left(z_{10}/10\right)}. \tag{15}$$

Moreover, at sea level, the air density has an approximate value of 1.225 kg/m^3. However, the air temperature at a specific region is not constant, because the site is an open space consisting of a mixture of dry air and a small amount of water vapor. The time varying air density at the considered heights is estimated using the below equation (Olaofe and Folly 2013):

$$\rho(h) = \frac{P_{av}}{RT_{av}}\exp\left(-\frac{gh}{RT}\right), \tag{16}$$

where $\rho(h)$ is the time varying air density as a function of height in kg/m^3, P_{av} is the average atmospheric pressure in hPa, R is the molar gas constant [287.05 J/(K mol)], T_{av} is the air temperature (K), g is the gravitational constant (9.81 m/s^2), and h is the considered height(s) above sea level.

Influence of ambient conditions on wind speed measurement

In general, there are several variables that can influence the wind speed measurement as discussed in Guerrero-Villar et al. (2019) and Danook et al. (2019). Guerrero-Villar et al. (2019) experimentally analyze the effect of temperature, humidity and atmospheric pressure on the cup anemometer behavior. Danook et al. (2019) studied the impact of relative humidity on the air density. The results indicated that humid air implies a lower density resulting in lower power from a wind turbine. Therefore, the aim of this section is to find the input parameter has the greatest influence in terms of affecting the prediction of wind speed in the selected region using an artificial neural network (ANN). To achieve this, seven parameters, namely maximum temperature, minimum temperature, maximum humidity, minimum humidity, Altimeter Pressure Settings, Atmospheric pressure at aerodrome elevation and number of days are considered as input parameters in the ANN models. To check the prediction accuracy using the identified parameters, 63 ANN models are developed.

Artificial neural network (ANN)

Artificial neural networks (ANNs) are known as potent nonlinear mathematical paradigms can be utilized to model the behavior of complex systems (Laqui et al. 2019). The

ANN aims to estimate the output value from input values by some internal calculations. ANNS have been adopted in several industrial and scientific fields (Kassem et al. 2019e). Feed-forward ANNs are the most practical types of artificial intelligence paradigms in approximating functions. ANN approaches consist of three types of layers called input, hidden and output layers. In the present study, nine parameters were selected for predicting daily wind speed, as shown in Table 1. Moreover, the structure of ANN used in this paper is shown in Fig. 4. In this study, the number of epochs and performance goal were 100,000 and 0.001, respectively. In addition, the number of hidden layers varied between 1 and 10, while the number of neurons varied between 5 and 50 s.

Table 1 Input and output variables

Parameters	Parameter description	Abbreviation
Input 1	Maximum temperature	Tmax
Input 2	Minimum temperature	Tmin
Input 3	Maximum humidity	Hmax
Input 4	Minimum humidity	Hmin
Input 5	Altimeter pressure settings	QNH
Input 6	Atmospheric pressure at aerodrome elevation	QFE
Input 7	Number of days	ND
Output 1	Wind speed	WS

Training and testing

The Levenberg–Marquardt (LM) algorithm is one of the most widely used and validated back-propagation algorithms. In general, the activation function for the neurons can be linear or non-linear. The logistic-sigmoid (*logsig*) and tangent-sigmoid (*tansig*) are used as activation functions whose outputs lie between 0 and 1 and are defined as

$$\log \text{sig} = \frac{1}{1+\mathrm{e}^{-x}}, \tag{17}$$

$$\text{tansig} = \frac{\mathrm{e}^{x}-\mathrm{e}^{-x}}{\mathrm{e}^{x}+\mathrm{e}^{-x}}. \tag{18}$$

The key step for developing an ANN is the training procedure, where the weights and biases are adjusted to minimize the difference between the output of the ANN and the actual value. To find the best performance for the ANN trained model, the mean squared error (MSE) is used. Equation (19) is used to normalize the data in the range of 0–1 and Eq. (20) is used to return the data to the original values after the simulation:

$$x_n = \frac{x_{\text{actual}} - x_{\min}}{x_{\max} - x_{\min}}, \tag{19}$$

$$x_{\text{actual}} = x_n\left(x_{\max} - x_{\min}\right) + x_{\min}. \tag{20}$$

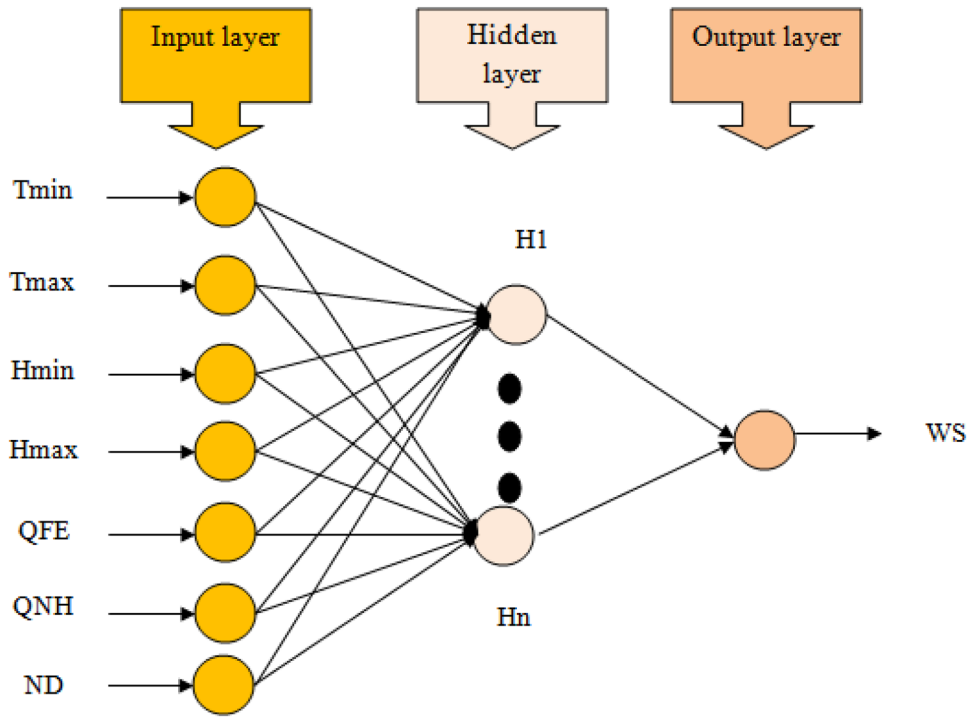

Fig. 4 Structure of ANN

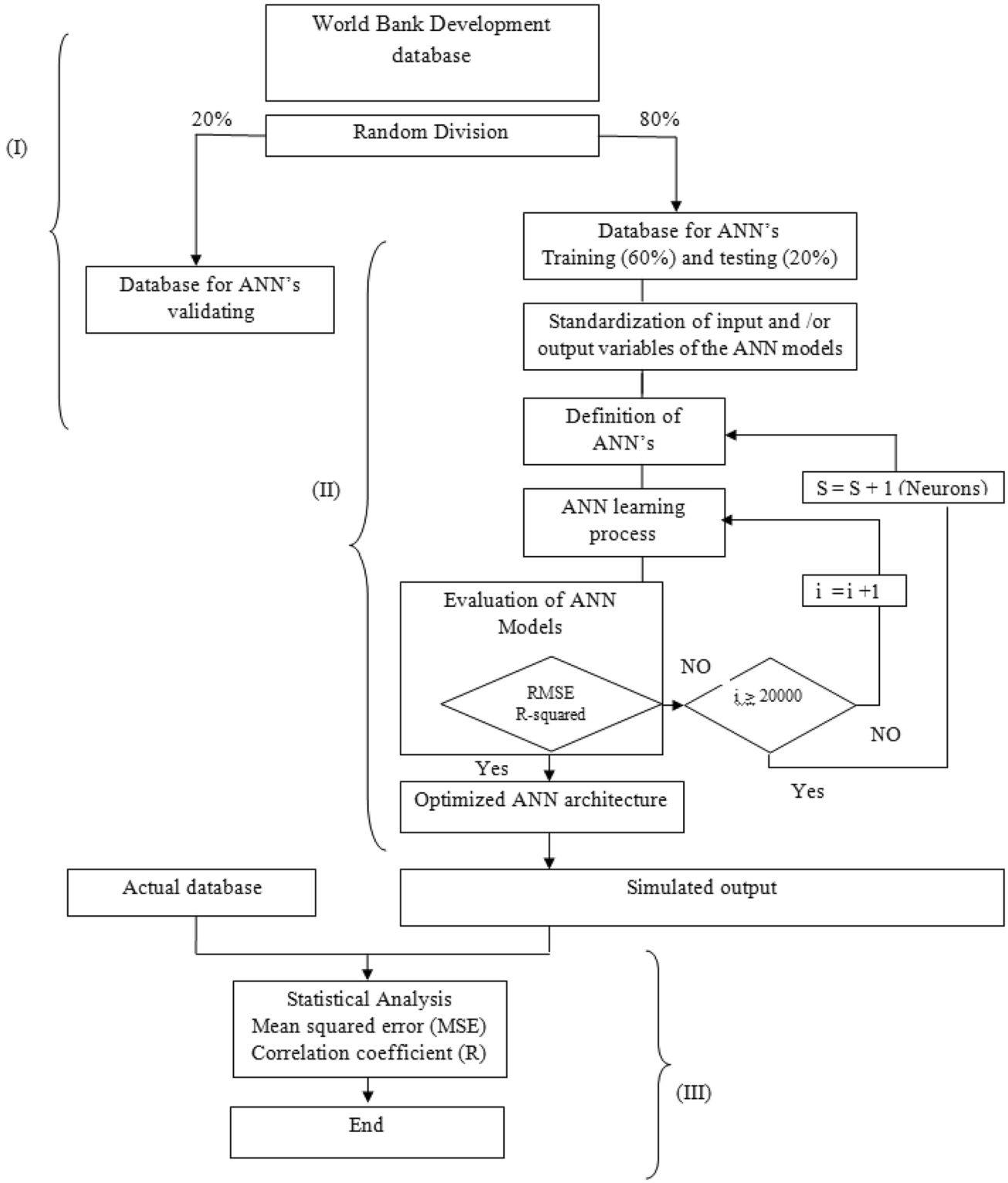

Fig. 5 Proposed ANN model for predicting the LUC and CP

Wind speed prediction with selected inputs

Figure 5 shows the methodology used in this study. In the present study, Tmin, Tmax, Hmin, Hmax, QFE and QNH are the inputs of the ANN models and WS is the output of the models. The optimum number of hidden layers and neurons are determined by a trial and error approach to obtain the best performance of the ANN model. In this research, 80% and 20% sets of training data and testing data were randomly selected, respectively. The testing data do not affect training and provide an independent measure of network performance during and after training. The developed models with different combination used to predict the wind speed of the selected regions are listed in Table 2.

Appraisal of the developed models

The developed ANN models were evaluated comprehensively to predict the monthly rainfall. The following statistical indicators were employed: mean squared error (MSE), root mean squared error (RMSE) and mean relative error (MAE):

$$R^2 = 1 - \frac{\sum_{i=1}^{n} \left(a_{a,i} - a_{p,i}\right)^2}{\sum_{i=1}^{n} \left(a_{p,i} - a_{a,\text{ave}}\right)^2}, \tag{21}$$

$$\text{MSE} = \frac{1}{n} \sum_{i=1}^{n} \left(a_{a,i} - a_{p,i}\right)^2, \tag{22}$$

Table 2 ANN models developed in this study for predicting wind speed

No.	Number of inputs	No.	Number of inputs
ANN 1	Tmin	ANN 33	Tmin,Tmax, QNH
ANN 2	Tmax	ANN 34	Tmax, Hmin, Hmax
ANN 3	Hmin	ANN 35	Tmax, Hmin, ND
ANN 4	Hmax	ANN 36	Tmax, Hmin, QFE
ANN 5	ND	ANN 37	Tmax, Hmin, QNH
ANN 6	QFE	ANN 38	Hmin, Hmax, Day
ANN 7	QNH	ANN 39	Hmin, Hmax, QFE
ANN 8	Tmin, Tmax	ANN 40	Hmin, Hmax, QNH
ANN 9	Tmin, Hmin	ANN 41	Hmax, ND, QFE
ANN 10	Tmin, QFE	ANN 42	Hmax, ND, QNH
ANN 11	Tmin, QNH	ANN 43	Day, QFE, QNH
ANN 12	Tmin, Hmax	ANN 44	Tmin, Tmax, Hmin, Hmax
ANN 13	Tmin, ND	ANN 45	Tmin, Tmax, Hmin, ND
ANN 14	Tmax, Hmin	ANN 46	Tmin, Tmax, Hmin, QFE
ANN 15	Tmax, QFE	ANN 47	Tmin, Tmax, Hmin, QNH
ANN 16	Tmax, QNH	ANN 48	Tmax, Hmin, Hmax, ND
ANN 17	Tmax, Hmax	ANN 49	Tmax, Hmin, Hmax, QFE
ANN 18	Tmax, ND	ANN 50	Tmax, Hmin, Hmax, QNH
ANN 19	Hmin, QFE	ANN 51	Hmin, Hmax, ND, QFE
ANN 20	Hmin, Hmax	ANN 52	Hmin, Hmax, ND, QNH
ANN 21	Hmin, Day	ANN 53	Hmax, ND, QFE, QNH
ANN 22	Hmin, QNH	ANN 54	Tmin, Tmax, Hmin, Hmax, ND
ANN 23	Hmax, QFE	ANN 55	Tmin, Tmax, Hmin, Hmax, QFE
ANN 24	Hmax, Day	ANN 56	Tmin, Tmax, Hmin, Hmax, QNH
ANN 25	Hmax, QNH	ANN 57	Tmax, Hmin, Hmax, ND, QFE
ANN 26	QFE, ND	ANN 58	Tmax, Hmin, Hmax, ND, QNH
ANN 27	QNH, Day	ANN 59	Hmin, Hmax, ND, QFE, QNH
ANN 28	QFE, QNH	ANN 60	Tmin, Tmax, Hmin, Hmax, ND, QFE
ANN 29	Tmin, Tmax, Hmin	ANN 61	Tmin, Tmax, Hmin, Hmax, ND, QNH
ANN 30	Tmin, Tmax, Hmax	ANN 62	Tmax, Hmin, Hmax, ND, QFE, QNH
ANN 31	Tmin, Tmax, ND	ANN 63	Tmin, Tmax, Hmin, Hmax, ND, QFE, QNH
ANN 32	Tmin, Tmax, QFE		

$$\mathrm{RMSE} = \sqrt{\frac{1}{n}\sum_{i=1}^{n}\left(a_{a,i} - a_{p,i}\right)^2}, \tag{23}$$

where n is the number of data, $a_{p,i}$ is the predicted values, $a_{a,i}$ is the actual values, $a_{\mathrm{a,ave}}$ is the average actual values and i is the number of input variables.

Description and design of the wind or PV project

Description and design of the wind power project

It is not possible to convert all the power produced by the wind turbine into electrical power. Power conditioning, a transmission mechanism, and rotor are significant parameters that affect the electrical power (Alsaad 2013). The theoretical power of the wind, P is given as

$$P = \frac{1}{2}\rho A v^3 = \frac{1}{2}\rho\left(\frac{\pi}{4}d^2\right)v^3, \tag{24}$$

where ρ is the air density ($\rho = 1.25$ kg/m^3), d is the rotor diameter in m, and v is the wind speed of the region. Using Eq. (24), the power produced from the wind becomes

$$P = \frac{\pi}{8}\rho d^2 v^3 = \frac{1}{2}d^2 v^3. \tag{25}$$

According to Alsaad (2013), the efficiency value for the power conditioning is about 90%, the transmission system is 40%, and the rotor ranges from 35 to 40%. Therefore, the total efficiency ranges from 13 to 15%, which is the result of multiplying all efficiencies of the power conditioning, transmission mechanism, and rotor.

Thus, a coefficient called Hugh's coefficient (C_H) must be included in Eq. (25) to determine the actual wind power. As a result, the actual wind power can be estimated using Eq. (26) (Alsaad 2013):

$$P = C_H d^2 v^3. \tag{26}$$

In general, wind speed is the most important factor that affects the amount of electricity produced from the wind turbine. Therefore, designing a wind farm in a specific region depends on the wind speed and wind turbine characteristics. This theoretical design is used to obtain the nominal capital cost, which can help in conducting a feasibility study for the present research. Moreover, the amount of the time that the wind farm project is able to generate electricity over an specific period of time investigated divided by the total amount of available time during the period is called the availability factor (AF). For the wind turbine, the availability is determined by deducting the time intervals where speed of the wind is lower than cut-in or higher than the cut-out speeds of the wind turbine. The AF is defined as (Alsaad 2013):

$$\mathrm{AF} = 1 - \frac{n}{N}, \tag{27}$$

where n is the number of months when the wind speed is lower than the specified cut-in speed and N is the total number of months during the investigation period.

In this study, the selected wind turbine, AN BONUS 1 MW—70 m with a capacity of 1000 kW is selected after an overall comparison of various wind turbine types. The selected wind turbine that satisfies the estimated annual energy for the selected location is shown in Table 3.

Description and design of the solar PV project

Lebanon has to make an important decision regarding its energy infrastructure in the coming years, especially in the power sector. In addition, Lebanon has tremendous scope for generating solar energy. Based on the global solar atlas map, it is found that the annual average of GHI of Lebanon varies from 1680 to 2118 kWh/m^2. The highest global horizontal irradiation is in the western part of Lebanon, which ranges from 5.4 to 5.8 kWh/m^2/day. Furthermore, it is noticed that the annual DNI values of the western part of Lebanon are within the range of 6.4–7.2 kWh/m^2/day. These results indicate that Lebanon has huge solar energy potential for assessing the energy generation for PV/flat-plate photovoltaic, CSP and CPV technologies. In addition, air temperature (TEMP) is considered as the second important parameter for evaluating the performance of solar PV systems. Based on the global solar atlas map, it is observed that the air temperature values vary from 5.3 to 21.9 °C. It can be concluded that

Table 3 Specifications of wind turbine

Parameter	Unit	Value
Power capacity per turbine	kW	1000
Manufacture	Siemens	–
Model	AN BONUS 1 MW—70 m	
Number of turbines	–	100
Hub height	M	70
Rotor diameter per turbine	M	54.2
Swept area per turbine	m^2	2307.22
Cut-in wind speed	m/s	3.0
Rated wind speed	m/s	15.0
Cut-out wind speed	m/s	25.0
Number of blades	–	3
Shape factor	–	2
Array losses	%	3
Airfoil losses	%	2
Miscellaneous losses	%	3
Availability	%	98

Lebanon has huge solar potential and it can be used to generate power, i.e., the PV output power is within the range of 3.99–5.30 kWh/kWp according to the global solar atlas map. In general, the global solar atlas map is the most reliable source of data currently available that is used to estimate the solar potential in the specific region. It is sufficient for the first step in the decision-making process in terms of the proposed solar PV project in the country. Furthermore, in solar PV project development stage, meteorological data are required for the technical design, engineering, financing, risk assessment, and due-diligence.

In this section, NASA average monthly global solar data are used to evaluate the solar potential for the selected region in Lebanon. In addition, the technical specifications of solar PV system, design methodology, and parameters are discussed in detail in Kassem et al. (2020).

Power generating factor The power generation factor (PGF) is an important factor that must be considered in the sizing of solar photovoltaic technology based on the total watt peak rating of the system. The PGF is calculated using the below equation:

$$\text{PGE} = \frac{\text{Solar irradiance} \times \text{Sunshine hours}}{\text{Standard test condition irradiance}}. \tag{28}$$

Energy demand The total power and energy consumption of all loads that will be supplied by the system for the selected location are essential factors needed to design a solar PV system.

Solar PV energy required The energy that must be generated by the PV module is the total Watt-hour per day needed from the PV modules and it is calculated using Eq. (29):

$$\text{The energy required from PV modules} = \text{Peak energy requirement} \times \text{Energy lost in the system}. \tag{29}$$

PV module sizing To calculate the size of the photovoltaic modules that are required, it is first necessary to estimate the total Watt-peak rating needed for the PV modules using the formula below:

$$\text{Total Watt peak rating} = \frac{\text{Solar PV energy required}}{\text{panel generation factor}}, \tag{30}$$

$$\text{PV module size} = \frac{\text{Total Watt peak rating}}{\text{PV output power rating}}. \tag{31}$$

Inverter sizing The size of an inverter used for any solar photovoltaic project is a function of the total wattage of the energy consumed and the factor of safety, and it is calculated as shown below:

$$\text{Inverter size} = \text{Peak energy requirement} \times \text{Factor of safety}. \tag{32}$$

A 100 MW photovoltaic solar system is proposed for the project to power the selected location. The Canadian Solar mono-Si-CS6X-300 M, details of which are given in Table 5, was considered because of its availability and cost-effectiveness for the Lebanese market when compared to other solar PV modules. Thus, to build the 100 MW grid-connected PV plant in the suitable region, 333,333 modules are required. The Canadian Solar mono-Si-CS6X-300 M, details of which are given in Table 4, was considered because of its availability and cost-effectiveness in the Lebanese market when compared to other solar PV modules. Moreover, the proposed inverter for the 100 MW solar power plant is a GE

Table 4 Technical details of the Canadian Solar mono-Si-CS6X-300 M

Parameters	Unit	Value
Type	Mono	–
Frame area	m^2	1.919
Watts (STC)	W	300
Watts (PTC)	W	217
Max power voltage (VMPP)	V	36.5
Max power current (IMPP)	A	8.22
Open circuit voltage (VOC)	V	45.0
Short circuit current (ISC)	A	8.74
Max system voltage (UL)	V	DC 600
Efficiency	%	15.63

Table 5 Technical details of the GE power conversion: brilliance inverter

Parameter	Unit	Value
PV array power range input	kWp	1300
Voltage range MPPT	V	200–850
Max voltage DC	V	1000
Max current	A	2400
Number of DC inputs	–	14
Peak efficiency	%	98.6
Efficiency: CEC wtd	%	98.4
Rated power output	kW	1262
Max current	A	1536
Rated voltages	V	480
Frequency	Hz	50/60
Operating range	°C	− 30 to 60

Power Conversion: Brilliance inverter (the specifications of the used inverter are shown in Table 5).

Economic analysis

RETScreen Expert software is used in this study to evaluate the technical, economic and environmental aspects of the proposed wind/PV projects and to compare its potential between selected regions. Several researchers have worked on designing a wind/PV system using RETScreen to estimate the potential and viability of renewable projects, especially those involving wind and solar (Owolabi et al. 2019; Rafique et al. 2018; Kassem et al. 2020). RETScreen Expert software is also capable of estimating annual and monthly energy productions, capacity factors, and other important economic measures, which are defined as an equation given below:

Net present value (NPV)

$$\mathrm{NPV} = \sum_{n=0}^{N} \frac{C_n}{(1+r)^n}. \tag{33}$$

Levelized cost of energy (LCOE)

$$\mathrm{LCOE} = \frac{\text{sum of cost over lifetime}}{\text{s of electricity generated over the lifetime}}. \tag{34}$$

The internal rate of return (IRR)

$$O = \sum_{n=0}^{N} \frac{C_n}{(1+\mathrm{IRR})^n}. \tag{35}$$

Simple payback (SP)

$$\mathrm{SP} = \frac{C - \mathrm{IG}}{\left(C_{\mathrm{ener}} + C_{\mathrm{capa}} + C_{\mathrm{RE}} + C_{\mathrm{GHG}}\right) - \left(C_{o\&M} + C_{\mathrm{fuel}}\right)}. \tag{36}$$

Equity payback (EP)

$$\mathrm{EP} = \sum_{n=0}^{N} C_n. \tag{37}$$

Annual life cycle savings (ALCS)

$$\mathrm{ALCS} = \frac{\mathrm{NPV}}{\frac{1}{r}\left(1 - \frac{1}{(1+r)^N}\right)}. \tag{38}$$

GHG emission reduction cost (GHGERC)

$$\mathrm{GHGERC} = \frac{\mathrm{ALCS}}{\Delta_{\mathrm{GHG}}}. \tag{39}$$

Capacity factor (CF)

$$\mathrm{CF} = \frac{P_{\mathrm{out}}}{P \times 8760}. \tag{40}$$

Results and discussion

In this study, the characteristics of wind speed and energy potential in Rayak region, Lebanon were investigated using 11 years of wind speed measured at a height of 10 m. In addition, the wind power and energy densities were calculated at various heights to classify the wind power at the selected location. In addition, ANN models were used to identify the most significant meteorological parameters that affect the wind speed measurement. Moreover, a feasibility study of a 100 MW grid-connected wind/solar project was conducted using RETScreen Expert software. The following section presents a discussion of the results obtained.

Wind energy potential and identifying the most significant input parameters for predicting wind speed

Wind speed characteristics and wind energy potential

Figure 6 shows the seasonal daily variation of wind speed for the 11 years (1996–2006) at the selected location. It can be seen that the maximum and minimum values of wind speed during the investigation period are 9.089 m/s and 1.372 m/s, respectively. In addition, it is observed that the higher wind speeds occur in the autumn season and the minimum wind speed occurs in winter season. Moreover, the annual daily variation in wind speed during the investigation period is shown in Fig. 7. It is found that the minimum and maximum wind speeds range between 7.047 m/s and 4.201 m/s with an average value of 5.884 m/s. It is found that the highest and lowest wind speeds were recorded in 1996 and 2001, respectively. The mean annual wind speed for 1996–2006 is 5.884 m/s; therefore, it is concluded that the selected region has high wind resource potential.

Furthermore, Fig. 8 represents the annual season wind speeds for the 11 years along with their average for the

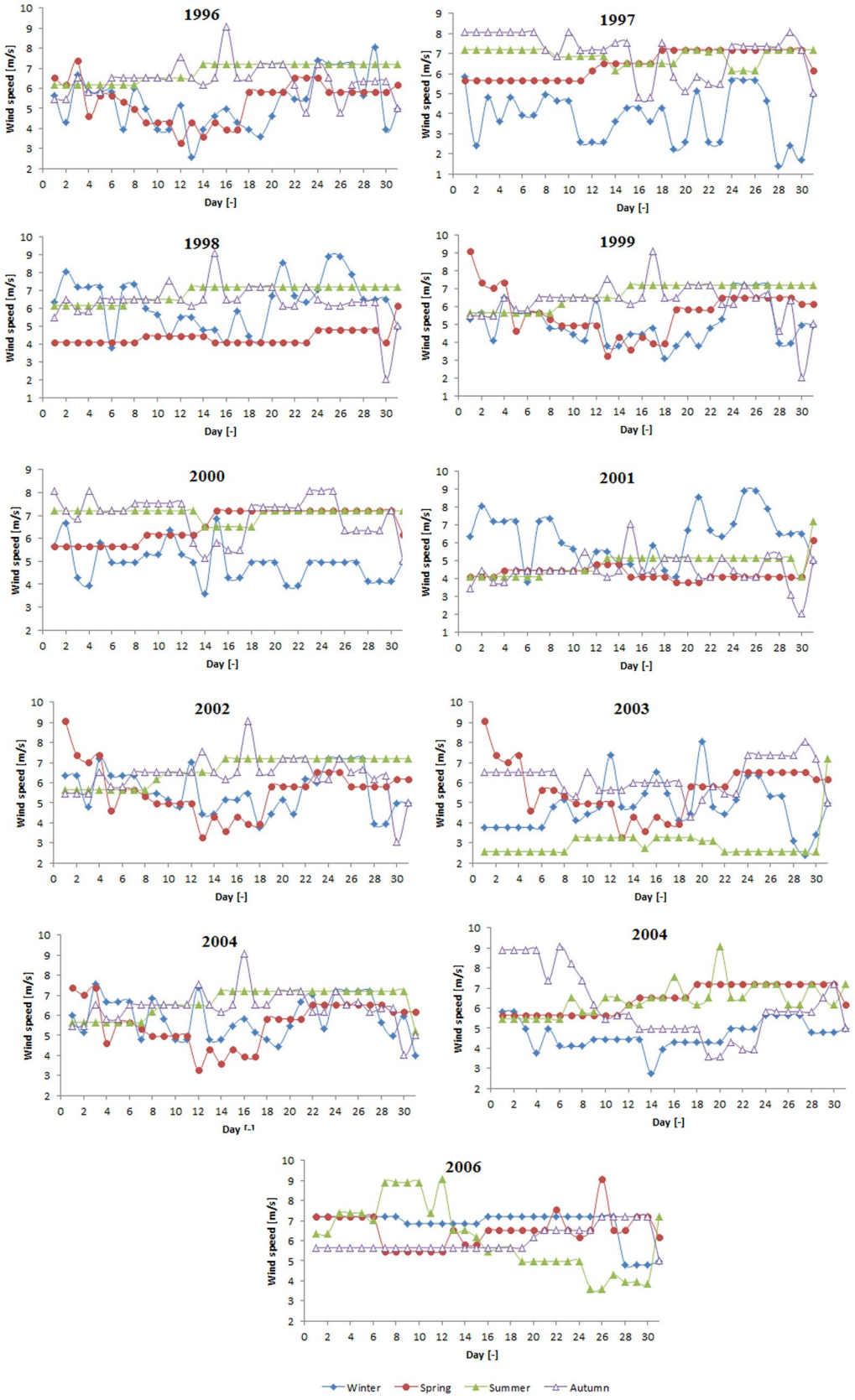

Fig. 6 Seasonal daily wind speed variations for each season

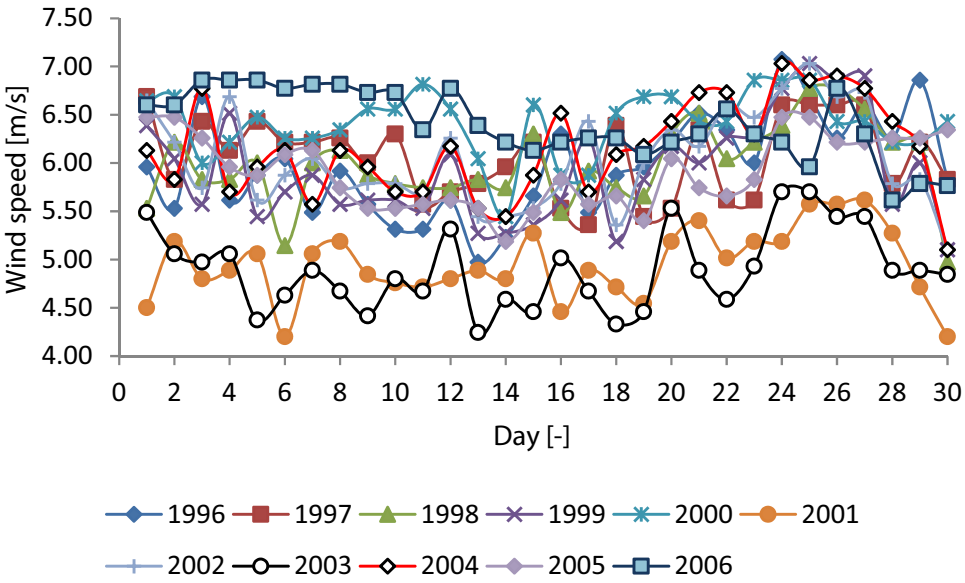

Fig. 7 Annual daily wind speed variation

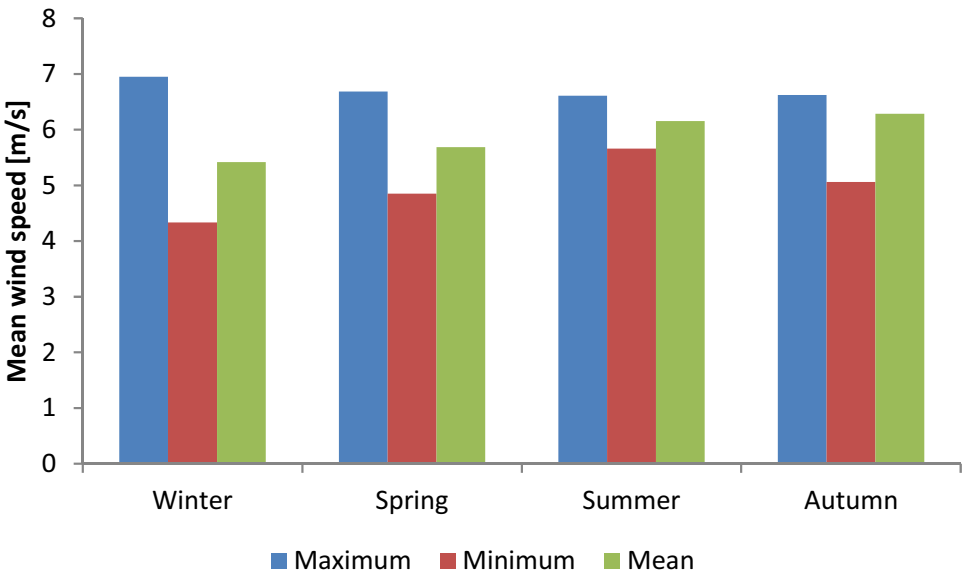

Fig. 8 Annual season wind speed for year (1996–2006)

specific location. The whole year is divided into four seasons: winter (December to February), spring (March to May), summer (from May to August) and autumn (September to November). It is found that the maximum wind speed of 6.953 m/s occurred in winter and the minimum value was also recorded in winter with a value of 4.334 m/s. In addition, it is observed that the highest mean wind speed of 6.284 m/s was recorded in autumn followed by summer and spring. Winter has the lowest mean wind speed with a value of 5.417 m/s.

To study the characteristics of the wind speed data, the Weibull probability distribution function was used. The wind speed frequency distribution, mean wind speed, and Weibull parameters have been calculated for the selected region. In addition, the most probable wind speed and the wind speed that carries the most energy were estimated by utilizing the parameters of the Weibull distribution function. Table 6 summarizes the seasonal and annual mean wind speed, standard deviation (SD), Weibull parameters and specific wind characteristics of the selected location for the period of 1996–2006. It is observed that the maximum and minimum values of shape parameter (k) are 22.853 in summer 2000 and 2.103 in autumn 1998, respectively. The value of k is above 2, which indicates that the wind speed was moderate to steady at a height of 10 m at the selected location. In addition, the k value for the 11 years was found to be 23.956. Moreover, the maximum scale parameter (c) was found to be 8.238 m/s

Table 6 Season, annual mean wind, standard deviation (SD), Weibull parameters, and specific wind characteristics for 1996–2006

Year	Parameter	Season				Average
		Winter	Spring	Summer	Autumn	
1996	Mean (m/s)	5.164	5.302	6.803	6.655	5.883
	SD (m/s)	1.309	1.1	0.585	3.062	0.565
	CV	0.253	0.207	0.086	0.46	0.096
	K	4.473	5.569	14.224	2.304	12.662
	c (m/s)	5.661	5.739	7.057	7.511	6.127
	V_{mp} (m/s)	5.35	5.54	7.02	5.87	6.09
	V_{maxE} (m/s)	6.15	6.06	7.12	9.85	6.20
1997	Mean (m/s)	3.776	6.448	6.879	7.299	5.988
	SD (m/s)	1.402	0.837	0.46	3.362	0.497
	CV	0.371	0.129	0.066	0.46	0.0831
	K	2.928	9.216	18.48	2.302	14.752
	c (m /s)	4.234	6.801	7.0813	8.238	6.204
	V_{mp} (m/s)	3.67	6.72	7.06	6.43	6.17
	V_{maxE} (m/s)	5.06	6.95	7.12	10.81	6.26
1998	Mean (m/s)	6.107	4.395	6.837	6.98	5.936
	SD (m/s)	2.023	0.578	0.573	3.486	0.4604
	CV	0.331	0.131	0.0838	0.499	0.077
	K	3.325	9.091	14.618	2.103	15.843
	c (m /s)	6.806	4.64	7.086	7.881	6.137
	V_{mp} (m/s)	6.11	4.58	7.05	5.80	6.11
	V_{maxE} (m/s)	7.84	4.74	7.15	10.83	6.18
1999	Mean (m/s)	4.961	5.577	6.635	6.508	5.839
	SD (m/s)	1.138	1.233	0.823	3.115	0.584
	CV	0.229	0.221	0.124	0.478	0.099
	K	4.989	5.197	9.671	2.206	12.217
	c (m /s)	5.404	6.061	6.984	7.348	6.089
	V_{mp} (m/s)	5.17	5.82	6.91	5.59	6.05
	V_{maxE} (m/s)	5.78	6.45	7.12	9.84	6.17
2000	Mean (m/s)	4.85	6.554	7.08	7.08	6.331
	SD (m/s)	0.776	0.829	0.385	0.385	0.522
	CV	0.16	0.126	0.054	0.054	0.082
	K	7.369	9.471	22.853	22.853	14.859
	c (m /s)	5.171	6.905	7.25	7.25	6.559
	V_{mp} (m/s)	5.07	6.82	7.24	7.24	6.53
	V_{maxE} (m/s)	5.34	7.05	7.28	7.28	6.61
2001	Mean (m/s)	6.199	4.237	4.75	4.75	4.915
	SD (m/s)	1.453	0.333	0.575	0.575	0.387
	CV	0.234	0.0787	0.121	0.121	0.0789
	K	4.872	15.6	9.93	9.93	15.568
	c (m /s)	6.761	4.383	4.994	4.994	5.084
	V_{mp} (m/s)	6.45	4.36	4.94	4.94	5.06
	V_{maxE} (m/s)	7.26	4.42	5.09	5.09	5.12
2002	Mean (m/s)	5.535	5.461	6.615	6.433	6.008
	SD (m/s)	1.142	1.174	0.826	1.913	0.524
	CV	0.206	0.215	0.124	0.297	0.0872
	K	5.602	5.355	9.607	3.749	14.013
	c (m /s)	5.989	5.92	6.965	7.123	6.236
	V_{mp} (m/s)	5.78	5.70	6.89	6.56	6.20
	V_{maxE} (m/s)	6.32	6.28	7.10	7.98	6.30

Table 6 (continued)

Year	Parameter	Season				Average
		Winter	Spring	Summer	Autumn	
2003	Mean (m/s)	4.672	5.579	2.829	6.208	4.862
	SD (m/s)	1.158	1.245	0.432	0.864	0.437
	CV	0.247	0.224	0.152	0.139	0.09
	K	4.586	5.122	7.75	8.558	13.565
	c (m /s)	5.114	6.044	3.009	6.571	5.051
	V_{mp} (m/s)	4.85	5.79	2.96	6.48	5.02
	V_{maxE} (m/s)	5.53	6.45	3.10	6.73	5.10
2004	Mean (m/s)	5.854	5.516	6.667	6.476	6.108
	SD (m/s)	1.078	1.204	0.808	1.958	0.523
	CV	0.184	0.218	0.121	0.302	0.0856
	K	6.338	5.269	9.916	3.681	0.294
	c (m /s)	6.291	5.989	7.011	7.178	6.335
	V_{mp} (m/s)	6.12	5.75	6.94	6.59	6.30
	V_{maxE} (m/s)	6.57	6.37	7.14	8.08	6.39
2005	Mean (m/s)	4.625	6.458	6.305	5.989	5.885
	SD (m/s)	0.78	0.858	0.673	1.671	0.4108
	CV	0.168	0.132	0.1068	0.279	0.0698
	K	6.97	8.994	11.336	4.022	17.683
	c (m /s)	4.945	6.82	6.593	6.605	6.064
	V_{mp} (m/s)	4.84	6.73	6.54	6.15	6.04
	V_{maxE} (m/s)	5.13	6.97	6.69	7.30	6.10
2006	Mean (m/s)	6.9603	6.433	6.073	6	6.401
	SD (m/s)	1.055	0.759	1.713	0.764	0.383
	CV	0.151	0.118	0.282	0.127	0.059
	K	7.817	10.195	3.976	9.415	20.692
	c (m /s)	7.399	6.756	6.702	6.323	6.569
	V_{mp} (m/s)	7.27	6.69	6.23	6.25	6.55
	V_{maxE} (m/s)	7.62	6.88	7.43	6.45	6.60
Annual	Mean (m/s)	5.353	5.644	6.133	6.264	5.857
	SD (m/s)	0.728	0.634	0.288	0.387	0.304
	CV	0.136	0.112	0.047	0.061	052
	K	8.775	10.736	26.546	20.059	2956
	c (m /s)	5.659	5.915	6.262	6.434	5.992
	V_{mp} (m/s)	5.58	5.86	6.25	6.42	5.98
	V_{maxE} (m/s)	5.79	6.01	6.28	6.46	6.01

in autumn 1997 and 3.009 in summer 2003. Furthermore, it is observed that the V_{mp} and V_{maxE} values ranged from 7.27 to 3.67 m/s and 10.83 to 3.10 m/s, respectively. In addition, the maximum value of V_{mp} and V_{maxE} was estimated at 7.27 m/s in winter 2006 and 10.83 m/s in autumn 1998. The V_{mp} and V_{maxE} for the 11 years were 5.98 m/s and 6.01 m/s, respectively, which is almost the same. The probability density functions and cumulative density functions with real data histograms are presented in Fig. 9 for 1996–2006.

Moreover, it is important to discuss the output generated by the wind in the form of power density. The seasonal air density at various heights was calculated using Eq. (16) and ranged from 1.171 to 1.245 kg/m^3. In addition, the average annual air density of the selected location was found to be 1.221 kg/m^3 at a height of 10 m. A similar result was found by Olaofe and Folly (2013). They found that the average air density of Darling City was 1.222 kg/m^3 at a height of 10 m. After calculating the density at a height of 10 m, Eq. (10) was used to calculate the wind power density at that height and the results are listed

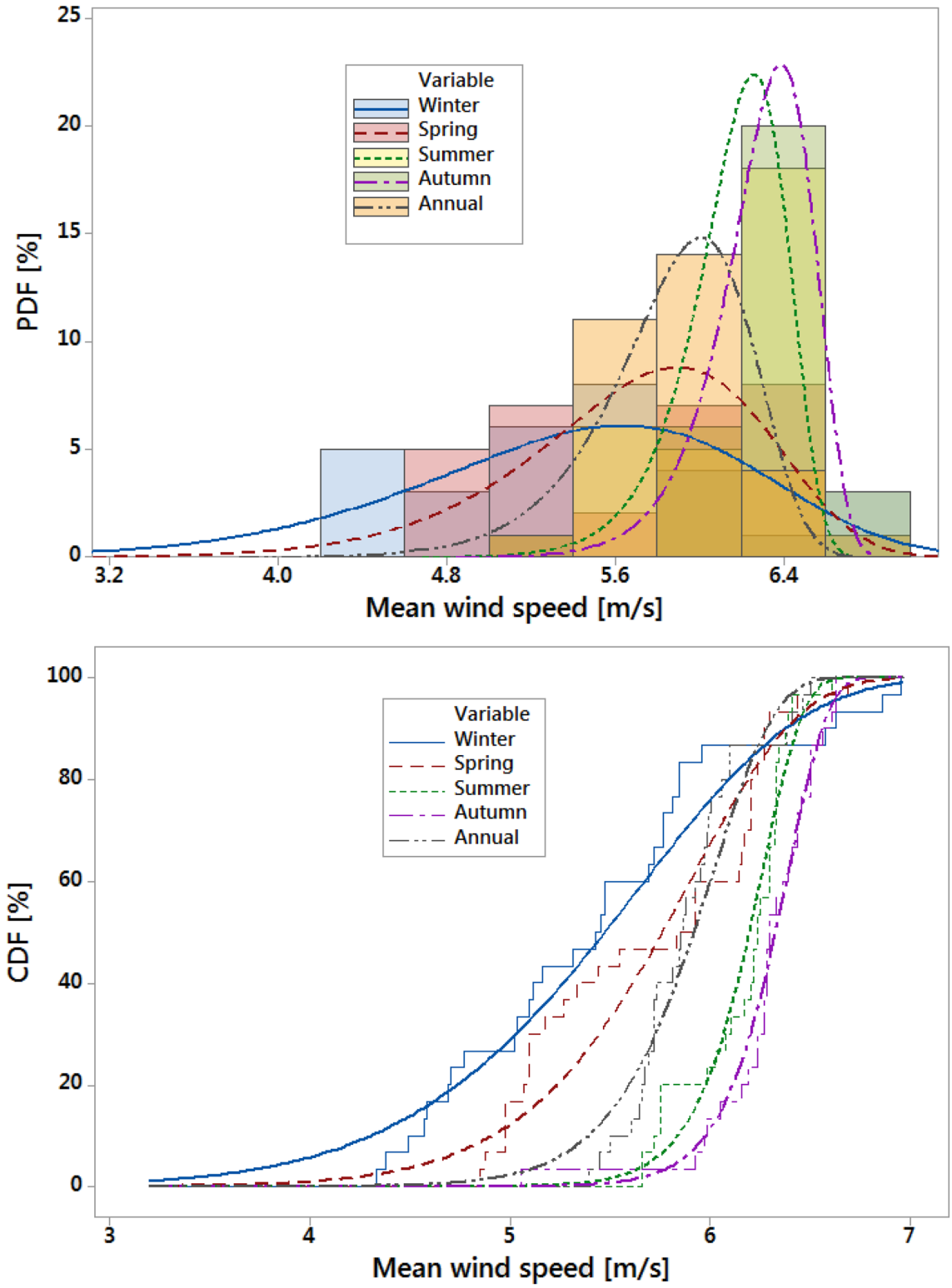

Fig. 9 Wind speed frequency distribution analysis for 1996–2006

in Table 7. It is found that the maximum and minimum actual wind power density values occurred in the summers of 2000 and 2003 with values of 217.389 W/m^2 and 13.997 W/m^2, respectively. In addition, it is noticed that the average annual wind speed for the period 1996–2006 was found to be 124.534 W/m^2. The wind energy potential

Table 7 Season and annual wind power density

Year	Season	Actual (W/m^2)	Estimated (W/m^2)	Error (%)	Year	Season	Actual (W/m^2)	Estimated (W/m^2)	Error (%)
1996	Winter	89.365	84.071	5.924	2002	Winter	107.313	103.523	3.531
	Spring	93.198	90.992	2.367		Spring	106.657	99.427	6.779
	Summer	193.108	192.215	0.463		Summer	178.892	176.716	1.217
	Autumn	163.644	179.941	9.959		Autumn	161.405	162.527	0.695
	Average	129.833	124.303	4.259		Average	136.069	132.396	2.699
1997	Winter	33.079	32.869	0.635	2003	Winter	67.097	62.258	7.212
	Spring	166.709	163.667	1.825		Spring	111.978	106.012	5.328
	Summer	199.696	198.729	0.484		Summer	13.997	13.822	1.249
	Autumn	216.339	237.397	9.734		Autumn	151.344	146.063	3.489
	Average	135.836	131.078	3.502		Average	71.765	70.167	2.228
1998	Winter	155.513	139.049	10.587	2004	Winter	128.562	122.474	4.736
	Spring	49.265	51.828	5.202		Spring	106.330	102.461	3.639
	Summer	196.039	195.111	0.473		Summer	183.081	180.916	1.182
	Autumn	161.909	207.612	28.227		Autumn	166.121	165.808	0.188
	Average	130.768	127.693	2.351		Average	143.878	139.118	3.309
1999	Winter	78.231	74.541	4.717	2005	Winter	62.178	60.398	2.864
	Spring	111.978	105.898	5.429		Spring	166.709	164.430	1.368
	Summer	178.892	178.323	0.318		Summer	160.616	153.017	4.731
	Autumn	155.093	168.278	8.502		Autumn	138.116	131.144	5.048
	Average	126.964	121.535	4.276		Average	126.322	124.430	1.498
2000	Winter	72.775	69.648	4.296	2006	Winter	198.999	205.859	3.447
	Spring	175.223	171.872	1.912		Spring	172.053	162.527	5.537
	Summer	217.389	216.663	0.334		Summer	138.700	136.740	1.413
	Autumn	212.172	216.663	2.117		Autumn	136.953	131.868	3.713
	Average	160.724	154.918	3.612		Average	160.348	160.114	0.146
2001	Winter	155.513	145.429	6.485	Annual	Winter	97.051	93.643	3.511
	Spring	46.578	46.437	0.304		Spring	112.378	109.761	2.329
	Summer	65.666	65.428	0.362		Summer	142.469	140.833	1.148
	Autumn	54.316	65.428	20.459		Autumn	151.513	150.052	0.964
	Average	74.050	72.486	2.112		Average	124.534	122.662	1.503

Table 8 Wind power classification at the 10 m height (Ilinca et al. 2003)

Powe class	Wind power density (W/m^2)
1 (poor)	≤ 100
2 (marginal)	≤ 150
3 (moderate)	≤ 200
4 (good)	≤ 250
5 (excellent)	≤ 300
6 (excellent)	≤ 400
7 (excellent)	≤ 1000

Table 9 Wind power classification at the 10 m height (Fazelpour et al. 2017)

Classification	Wind power density range (W/m^2)
Fair	$P/A < 100$ W/m^2
Fairly good	$100 \le P/A < 300$ W/m^2
Good	$300 \le P/A < 700$ W/m^2
Very good	$P/A \ge 700$ W/m^2

classification according to the value of wind power density is presented in Table 8. From these results, it observed that the selected region could be considered as class 2, which indicates marginal wind power potential. In addition, according to Fazelpour et al. (2017), the wind density of the selected location is classified as fairly good, as shown in Table 9.

Figure 10 illustrates the seasonal wind speed and wind power density for 1996–2006. According to the wind power classification, the winter season is in class 1 as the actual and calculated wind power density is less than 100 W/m^2, whereas the spring and summer seasons are

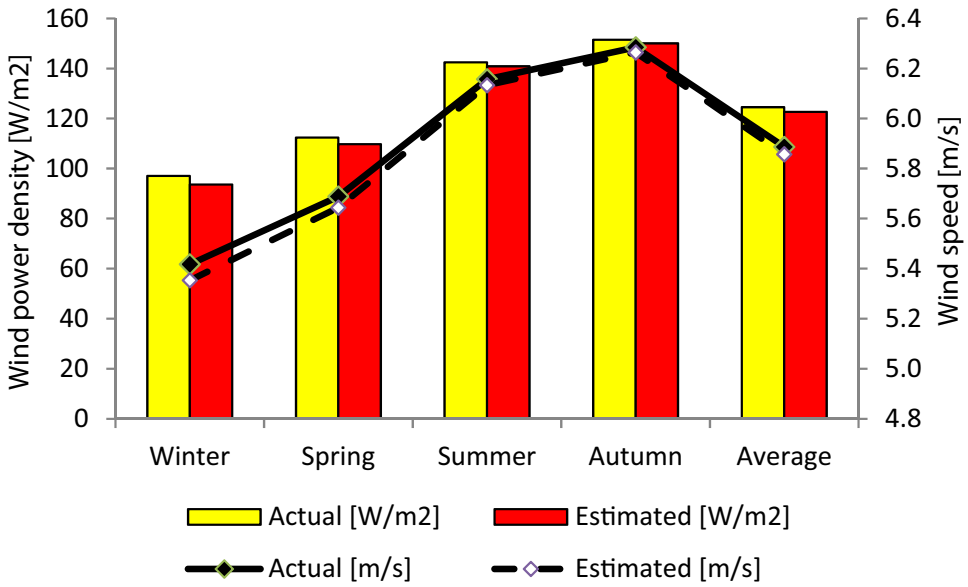

Fig. 10 Seasonal wind speed and wind power density for 1996–2006

in class 2. Finally, the autumn season is in class 3 as the calculated power density is greater than 150 W/m^2.

Most influential variables for predicting wind speed

Forecasting of wind speed is essential for designing a wind project, and projected potential future wind system feasibility. Therefore, several meteorological variables are used to determine the most effective variables for wind speed prediction. In the present study, 63 ANN models with different input combinations are evaluated for the prediction of WS. All the models are validated against the actual data of the WS based on statistical measures such as RMSE and MSE. For higher modeling accuracy, RMSE indices should be closer to zero. MATLAB 2015a was used to train and test the developed ANN models. To select the best architecture of the developed ANN model, the numbers of hidden layers and neurons were varied. The network with the minimum MSE invalidation is called the trained ANN model. The best performance of the network was obtained by training the developed ANN architecture several times until the MSE showed the minimum value. The same-trained network was tested with the new datasets to check the performance of the network. The numbers of neurons started from 1 and were constantly increased and re-training of the ANN continued until the satisfactory then is considered as the optimal number. Table 10 shows the optimum number of hidden layers and neurons and the activation function that was chosen for each ANN model. 63 ANN models (ANN1 to ANN36) were developed with different input combination and the target for all the models is daily WS.

Case 1: parameter selection for 1 input (ANN1–ANN7)

It is found that ND gave the best performance followed by Tmin for estimating the WS. Moreover, it is observed that the lowest performance was obtained from QNH with RMSE of 0.2221.

Case 2: parameter selection for 2 input (ANN8–ANN28)

21 possible combinations were considered and analyzed to find the best integration of 2 parameters. It is found that the lowest RMSE was recorded for the combinations of ANN 27 [QNH, ND] and the highest RMSE was obtained from the combinations of ANN 24 [Hmax, ND] for estimation of the daily WS.

Case 3: parameter selection for 3 input (ANN29–ANN43)

In this case, three parameters were considered as inputs. For this purpose, 15 ANN models were developed to evaluate the importance of each input variable and identify the most relevant input. The ANN 43 with a combination of [ND, QFE, QNH] produced the lowest RMSE and ANN 34 with a combination of [Tmax, Hmin, Hmax] gave the highest RMSE.

Case 4: parameter selection for 4 input (ANN44–ANN53)

In this case, the test was performed to select the most important sets combined of 4 input parameters. To achieve this, 10 different combinations of 4 inputs were considered to determine and introduce the most significant one for the prediction of daily WS. It is observed that the best combination for predicting daily WS was ANN 51 [Hmin, Hmax, Nd, QFE] with RMSE equal to 0.1583. In addition, it is found that the maximum RMSE was recorded for ANN 50 with

Table 10 Evaluation of the networks and Statistical tools' performance of the ANN model with a single input

Model	Number of hidden layer	Number of neuron	Transfer function	Epoch	Training			Testing	
					MSE	RMSE	AAD (%)	RMSE	AAD (%)
ANN 1	2	35	TANSIG	863	0,0419	0,2068	0,0147	0,2001	0,6954
ANN 2	3	60	TANSIG	921	0,0384	0,1986	0,0737	0,2015	0,5782
ANN 3	2	20	TANSIG	1000	0,0463	0,2251	0,1629	0,2204	0,6868
ANN 4	2	10	TANSIG	950	0,0494	0,2227	0,3062	0,2195	0,9928
ANN 5	2	60	TANSIG	339	0,0174	0,1280	0,2116	0,1382	0,3492
ANN 6	2	10	TANSIG	774	0,0483	0,2240	0,0809	0,2216	1,1309
ANN 7	2	40	TANSIG	1000	0,0478	0,2252	0,5259	0,2221	1,2573
ANN 8	2	30	TANSIG	88	0,0393	0,1870	0,1294	0,1936	0,7919
ANN 9	3	30	TANSIG	1000	0,0440	0,2063	0,2264	0,1985	0,3152
ANN 10	5	25	TANSIG	800	0,0479	0,2052	0,4184	0,1989	0,2707
ANN 11	4	50	TANSIG	416	0,0448	0,2034	0,4024	0,1983	1,1509
ANN 12	3	40	TANSIG	10	0,0401	0,1979	0,5523	0,1951	0,5555
ANN 13	3	30	TANSIG	67	0,0341	0,1765	0,0697	0,1855	0,6185
ANN 14	3	35	TANSIG	661	0,0404	0,2049	0,2747	0,2058	0,3284
ANN 15	2	65	TANSIG	573	0,0433	0,1952	0,1161	0,1935	1,0028
ANN 16	2	65	TANSIG	919	0,0432	0,1970	0,5516	0,2643	0,7531
ANN 17	2	5	TANSIG	125	0,0468	0,2204	0,0214	0,2165	0,8132
ANN 18	3	55	TANSIG	43	0,0352	0,1715	0,3757	0,1795	0,3619
ANN 19	2	10	TANSIG	872	0,0483	0,2240	0,2201	0,2189	1,0919
ANN 20	3	30	TANSIG	999	0,0523	0,2219	0,5235	0,2185	1,1713
ANN 21	2	70	TANSIG	913	0,0223	0,1400	0,0197	0,1541	0,7016
ANN 22	2	20	TANSIG	485	0,0513	0,2252	0,2799	0,2204	0,5988
ANN 23	2	15	TANSIG	367	0,0502	0,2205	0,2195	0,2189	1,1137
ANN 24	2	50	TANSIG	871	0,0214	0,1457	0,2262	0,5918	7,2142
ANN 25	2	15	TANSIG	839	0,0507	0,2242	0,4239	0,2200	1,1152
ANN 26	3	50	TANSIG	1000	0,0201	0,1431	0,2150	0,1556	0,7260
ANN 27	2	60	TANSIG	999	0,0250	0,1368	0,1561	0,1487	0,4453
ANN 28	3	40	TANSIG	549	0,0487	0,2240	0,0050	0,2208	0,9501
ANN 29	2	55	TANSIG	330	0,0338	0,1760	0,5127	0,1799	0,1021
ANN 30	2	55	TANSIG	915	0,0361	0,1629	0,2457	0,1785	0,5200
ANN 31	5	50	TANSIG	544	0,0266	0,1418	0,1615	0,1597	0,8027
ANN 32	3	70	TANSIG	172	0,0340	0,1677	0,4527	0,1741	0,2843
ANN 33	2	70	TANSIG	592	0,0340	0,1620	0,2038	0,1725	0,6657
ANN 34	3	40	TANSIG	824	0,0395	0,1873	0,0565	0,5370	5,4410
ANN 35	4	80	TANSIG	141	0,0322	0,1618	0,4793	0,1852	0,0635
ANN 36	3	90	TANSIG	562	0,0339	0,1932	0,1091	0,1956	1,0533
ANN 37	3	70	TANSIG	725	0,0452	0,1985	0,2815	0,2013	1,2213
ANN 38	2	75	TANSIG	974	0,0284	0,1523	0,0252	0,1693	0,2906
ANN 39	2	10	TANSIG	579	0,0441	0,2216	0,1379	0,2193	0,3498
ANN 40	2	10	TAN	435	0,0450	0,2217	0,1375	0,2193	0,3281
ANN 41	2	70	TAN	1000	0,0264	0,1431	0,1267	0,1622	0,4967
ANN 42	2	70	TAN	800	0,0213	0,1400	0,1843	0,1562	0,0215
ANN 43	2	55	TAN	929	0,0234	0,1391	0,3311	0,1522	0,2485
ANN 44	3	35	TAN	481	0,0358	0,1775	0,2425	0,1791	0,0468
ANN 45	2	50	TAN	125	0,0325	0,1568	0,0715	0,1804	0,3126
ANN 46	3	70	TAN	788	0,0345	0,1573	0,0375	0,1694	0,1312
ANN 47	2	70	TAN	655	0,0366	0,1608	0,2194	0,1828	0,8152
ANN 48	2	70	TAN	416	0,0285	0,1409	0,0241	0,1681	0,3911

Table 10 (continued)

Model	Number of hidden layer	Number of neuron	Transfer function	Epoch	Training			Testing	
					MSE	RMSE	AAD (%)	RMSE	AAD (%)
ANN 49	3	100	TAN	686	0,0356	0,1823	0,1407	0,1886	0,8556
ANN 50	2	120	TAN	1000	0,0452	0,1819	0,1799	0,6657	61,9212
ANN 51	3	70	TAN	793	0,0233	0,1392	0,0737	0,1583	0,2784
ANN 52	3	90	TAN	944	0,0281	0,1378	0,0874	0,1601	0,4457
ANN 53	2	50	TAN	999	0,0220	0,1351	0,3680	0,5468	20,9256
ANN 54	2	70	TAN	973	0,0187	0,1025	0,0476	0,1451	0,4125
ANN 55	3	70	TAN	195	0,0368	0,1698	0,2644	0,1797	0,2567
ANN 56	4	40	TAN	840	0,0311	0,1670	0,0513	0,1829	0,0492
ANN 57	2	90	TAN	50	0,0347	0,1720	0,0350	0,1786	0,0056
ANN 58	2	90	TAN	522	0,0324	0,1372	0,0051	0,1668	0,2270
ANN 59	3	90	TAN	829	0,0267	0,1365	0,0329	0,5326	10,4736
ANN 60	2	70	TAN	1000	0,0152	0,0949	0,3027	0,1235	0,5410
ANN 61	2	70	TAN	868	0,0127	0,0888	0,0831	0,1235	0,5410
ANN 62	3	90	TAN	654	0,0292	0,1273	0,0464	0,6257	27,1286
ANN 63	3	70	TAN	712	0,0183	0,1026	0,0859	0,1445	0,2528

a combination of [Hmin, Hmax, ND, QNH] for estimating daily WS.

Case 5: parameter selection for 5 input (ANN54–ANN59)

Six ANN models with five different combinations of inputs were developed to predict the daily WS. The ANN 54 tested with the combination of [Tmin, Tmax, Hmin, Hmax, ND] gave the lowest RMSE. In addition, it is noticed that the ANN 59 with the combination of [Hmin, Hmax, ND, QFE, QNH] produced the maximum RMSE value.

Case 6: parameter selection for 6 input (ANN60–ANN62)

In this case, the test was performed to select the most important sets combined of 6 input parameters. To achieve this, 3 different combinations of 6 inputs were considered to determine and introduce the most significant one for the prediction of daily WS. It is observed that the best combination for predicting daily WS was ANN 60 and ANN 61 with combinations of [Tmin, Tmax, Hmin, Hmax, ND, QFE] and [Tmain, Tmax, Hmin, Hmax, ND, QNH], respectively, with a value of 0.1235 for RMSE. In addition, it is found that the maximum RMSE was recorded for ANN 62 with a combination of [Tmax, Hmin, Hmax, ND, QFE, QNH] for estimating daily WS.

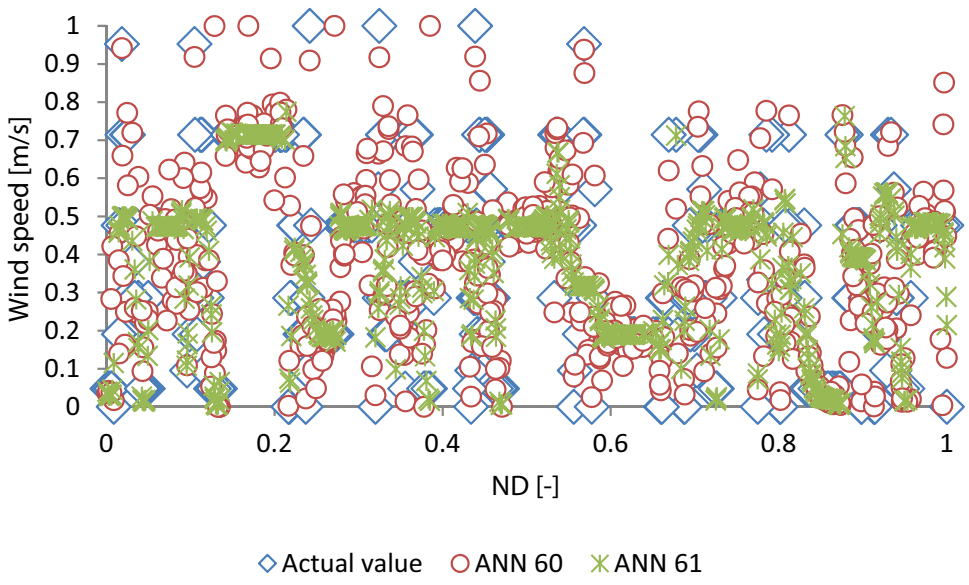

Fig. 11 Comparison between actual and predicting values by ANN 5 and ANN 60

Table 11 Rank of each ANN model

Rank	Model	RSME	Rank	Model	RSME	Rank	Model	RSME
1	ANN 60	0,1235	22	ANN 57	0,1786	4	ANN 14	0,2058
2	ANN 61	0,1235	23	ANN 44	0,1791	5	ANN 17	0,2165
3	ANN 5	0,1382	24	ANN 18	0,1795	6	ANN 20	0,2185
4	ANN 63	0,1445	25	ANN 55	0,1797	7	ANN 19	0,2189
5	ANN 54	0,1451	26	ANN 29	0,1799	8	ANN 23	0,2189
6	ANN 27	0,1487	27	ANN 45	0,1804	9	ANN 39	0,2193
7	ANN 43	0,1522	28	ANN 47	0,1828	10	ANN 40	0,2193
8	ANN 21	0,1541	29	ANN 56	0,1829	11	ANN 4	0,2195
9	ANN 26	0,1556	30	ANN 35	0,1852	12	ANN 25	0,2200
10	ANN 42	0,1562	31	ANN 13	0,1855	13	ANN 3	0,2204
11	ANN 51	0,1583	32	ANN 49	0,1886	14	ANN 22	0,2204
12	ANN 31	0,1597	33	ANN 15	0,1935	15	ANN 28	0,2208
13	ANN 52	0,1601	34	ANN 8	0,1936	16	ANN 6	0,2216
14	ANN 41	0,1622	35	ANN 12	0,1951	17	ANN 7	0,2221
15	ANN 58	0,1668	36	ANN 36	0,1956	18	ANN 16	0,2643
16	ANN 48	0,1681	37	ANN 11	0,1983	19	ANN 59	0,5326
17	ANN 38	0,1693	38	ANN 9	0,1985	20	ANN 34	0,5370
18	ANN 46	0,1694	39	ANN 10	0,1989	21	ANN 53	0,5468
19	ANN 33	0,1725	1	ANN 1	0,2001	22	ANN 24	0,5918
20	ANN 32	0,1741	2	ANN 37	0,2013	23	ANN 62	0,6257
21	ANN 30	0,1785	3	ANN 2	0,2015	24	ANN 50	0,6657

Case 7: parameter selection for 7 input (ANN63)

All seven input variables were applied to train and test the developed ANN, which was named ANN 63. The ANN-35 showed good prediction accuracy with an RMSE value of 0.1445.

Predicted daily WS values using the best input combination of all the ANN models are compared with the actual values, as shown in Fig. 11. The best combination of each ANN model is presented in Table 11. Out of the 63 ANN models, ANN 60, ANN61 and ANN 5 gave the best predictions with the combinations of [Tmin, Tmax, Hmin,Hmax, ND, QFE], [Hmin, Hmax, ND, QFE, QNH] and [ND], respectively. From the developed ANN models, the most relevant input variables for predicting the daily wind speed are found to be temperature in terms of maximum temperature and minimum temperature, pressure and relative humidity. In fact, measuring wind speed is necessary to calculate the annual energy production of a wind farm. Therefore, in the literature, several studies demonstrated that the air density influenced the power from a wind turbine (Danook et al. 2019; Yue et al. 2017; Guerrero-Villar et al. 2019; Ulazia et al. 2019). For example, Danook et al. (2019) found that the humid air implies lower density resulting in lower power from a wind turbine. Yue et al. (2017) concluded that at high temperatures, the high humidity effect on air density cannot be ignored for annual energy production calculations.

Solar energy potential

In general, two representative parameters including global horizontal irradiation (GHI) and direct normal irradiation (DNI) are used to analyze the global solar resources in the country. GHI and DNI are considered important parameters for assessing energy generation for PV/flat-plate photovoltaic technologies and the development of CSP (concentrating solar power) and CPV (concentrating photovoltaic) systems, respectively. As mentioned before, average monthly NASA data (2007–2016) were used to analyze the potential of solar energy in the selected region. Figure 12 illustrates the monthly solar irradiation in terms of GHI and DNI and the monthly mean air temperature values (AT) for the selected region. Based on the results, the monthly values of GHI ranged from 74.906 to 92.622 kWh/m^2. The maximum and minimum monthly values of GHI are recorded in July and December, respectively. Furthermore, it is found that the highest monthly DNI value of 249.565 kWh/m^2 was obtained in July. In addition, it is noticed that the maximum and minimum air temperature values were recorded in July and January with values of 23.28 °C and 8.55 °C for the selected region. Furthermore, the annual GHI and DNI were estimated to be 1877.41 kWh/m^2 and 1967.98 kWh/m^2, respectively. According to Prăvălie et al. (2019), it is found that the selected region has high solar resources and

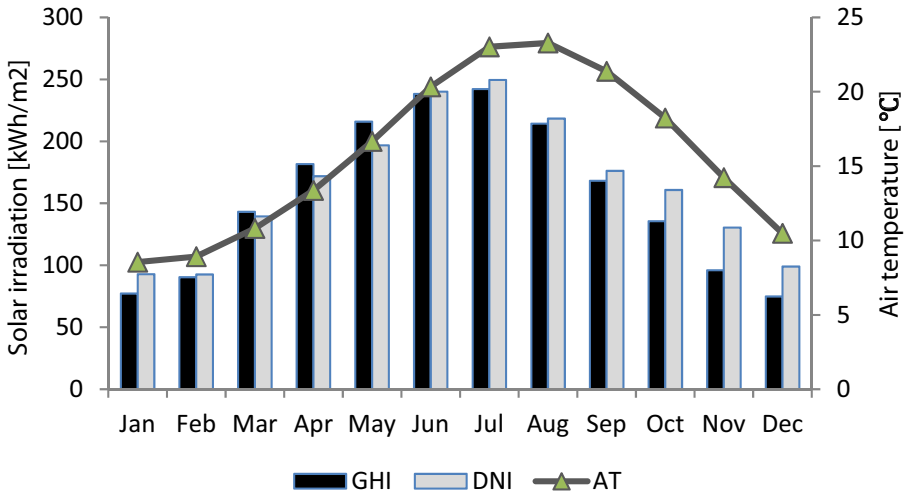

Fig. 12 Mean monthly GHI, DNI and AT for the selected region

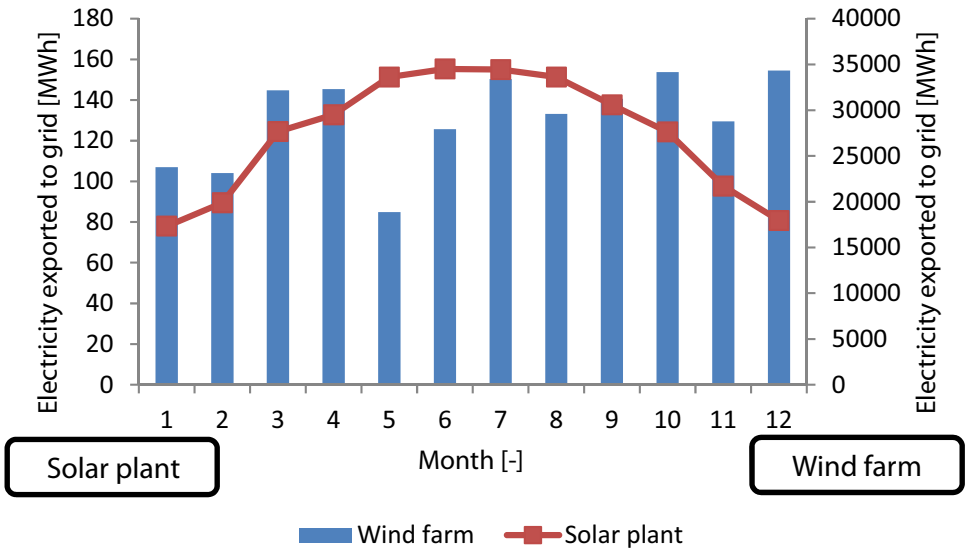

Fig. 13 Monthly power exported to grid for wind and solar projects

Table 12 Financial parameters

Factor	Unit	Value
Inflation rate	%	2
Discount rate	%	0
Reinvestment rate	%	9
Project life	year	25
Debt ratio	%	25
Dept interest rate	%	0
Dept term	year	20
Electricity export escalation rate	%	5

is categorized as having excellent potential. Consequently, it is concluded that the Rayak region is a suitable location for installing a large-scale photovoltaic system.

Comparative techno-economic assessment and environmental impacts of wind/solar projects

RETScreen software is used to investigate the feasibility of a 100 MW installed capacity wind farm and solar plant project in the selected region. In this section, a comparison between the two projects is made. Figure 13 presents the monthly results for the electricity generation from the installed projects. It is found that the highest electricity generation of 349717 MW is produced by the wind farm compared to the solar plant (i.e., 1478.053 MW). In addition, it is observed that the maximum electricity production was recorded in December for the wind farm and June for the solar farm. Moreover, the capacity factor of each project was 39.9% for the wind farm and 16.1% for the solar plant project.

The financial parameters of the proposed system seem to be economically feasible, as listed in Table 12. An overview of

the cash flow over the project life time for the wind farm and solar plant projects for the selected region is shown in Fig. 14. The cash flow indicates that investors are expected to receive a positive cash flow from year 8.6 onwards for the wind farm project and year 21.3 onwards for the solar plant project. A minimum equity payback of 6 years is observed for the wind farm project and 13.5 years for the solar plant project.

Moreover, the economic performance of the 100 MW installed capacity wind/solar project for the selected location is presented in Table 13. The results show that the proposed 100 MW wind farm project is very promising in the

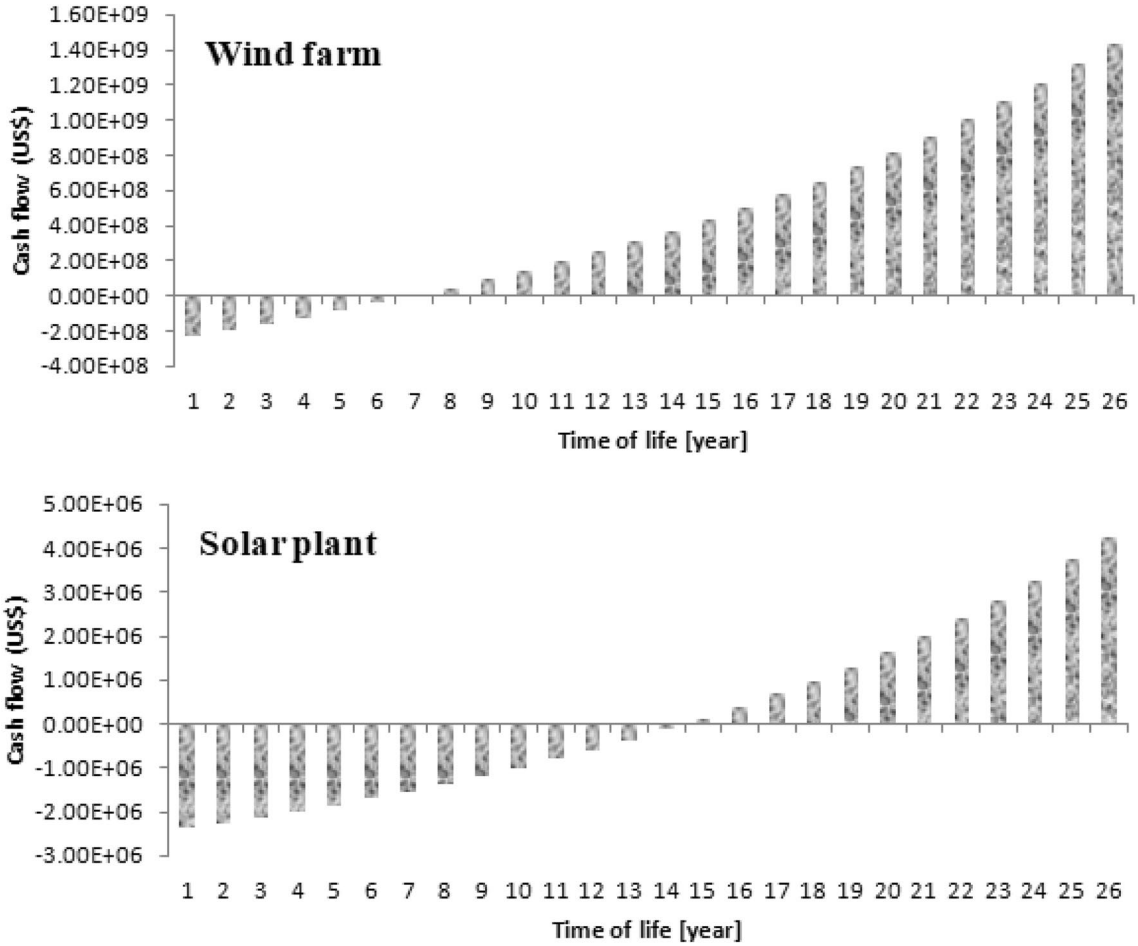

Fig. 14 Cumulative cash flow for all projects

Table 13 Performance of 100 MW installed capacity of wind farm and solar plant projects

Project	*NPV* ($)	*EP* (year)	*SP* (year)	*LCOE* ($/kWh]	*B-C*	*ALCS* ($/year)	*IRR-assets* (%)	*IRR-equity* (%)
Wind farm	14,440,093,149	6	8.6	0.035	7.4	57,603,726	15.2	19.3
Solar plant	4,257,044	13.5	21.3	0.085	2.8	170,282	5.1	7.5

Table 14 Net annual reduction of GHG emissions

Project	Net annual GHG emission reduction	Car and light trucks not used	People reducing energy use by 20%	Hectares of forest absorbing carbon
Wind farm	2,472,293	452,801	247,229.3	22,738.7
Solar plant	1044.9	191.4	1044.9	96.1

selected location due to the economic performance results obtained. Furthermore, the wind farm is a more economical option than the solar plant because of the higher values of NPV, BCR, ALCS, and IRR as well as the lower values of EB, SB and LCOE.

Greenhouse gas (GHG) emissions of the proposed renewable projects in terms of the total amount of annual GHG reduction in terms of tons of CO_2 per year (tCO_2/year) and cost ($/$tCO_2$) were estimated using RETScreen software. The utilization of wind energy as a partial replacement for traditional power production units in the country significantly reduces the emissions of GHG, as can be observed from Table 14. The obtained results demonstrate that a significant amount of CO_2 could be reduced by the proposed projects in the studied location. It can be observed that the total amount of CO_2 that can be reduced from the proposed projects was 245,472 tCO_2/year from the wind farm and 84,910,458 tCO_2/year from the PV plant. Generally, it can be concluded that the wind farm project reduce increased amounts of CO_2 emissions compared to the PV plant project.

Conclusion

Both population and industrial growth are causing significant increases in energy demand throughout over Lebanon, especially in terms of electricity demand, which means there is a considerable need to find alternative sources to replace the traditional energy sources produced by fossil fuels. Therefore, the present study was focused on wind and solar power potential assessment for the Rayak region in Lebanon.

For wind energy potential, the two-parameter Weibull distribution function is used to represent the wind speed distribution for the Rayak region in Lebanon. Wind speed data were collected from a measurement station in the Rayak area for an 11-year period measured at a height of 10 m. Yearly and seasonal parameters of the Weibull distribution function were estimated using the daily average wind speed data with the Maximum likelihood method. In addition, wind power density was calculated. For this purpose, the air density values were estimated using collected pressure and temperature values. As a result, the average annual wind speed for the years 1996–2006 was found to be 124.534 W/m^2, which could be considered as class 2 and indicates marginal wind power potential. Furthermore, the objective of the study was to predict the daily average wind speed using an Artificial Neural Network (ANN) approach. In this study, 63 ANN models were developed by varying the weather parameters. An 11-year database comprising daily wind speed, minimum temperature, maximum temperature, minimum relative humidity, maximum relative humidity, altimeter Pressure Settings and atmospheric pressure at aerodrome elevation were used in the ANN models. All the models were validated and the performances of the models were analyzed. Out of the 63 ANN models, ANN 60, ANN61 and ANN 5 gave the best prediction with the combinations of [Tmin, Tmax, Hmin, Hmax, ND, QFE], [Hmin, Hmax, ND, QFE, QNH] and [ND], respectively. Besides, for the future installation of PV, the solar energy potential of the selected location was assessed using NASA's average monthly solar radiation. The results indicated that Rayak region has high solar resources and are categorized as excellent. Consequently, it is concluded that Rayak region is a suitable location for installing large-scale photovoltaic systems.

Moreover, the purpose of the present study is to evaluate the feasibility of developing 100 MW grid-connected wind/PV power project in the selected region. To fulfil this objective, RETScreen Expert software was used to validate the techno-economic and environmental sustainability of installing a grid-connected wind and PV system in the country. mono-Si-CS6X-300 M module manufactured by Canadian Solar and AN BONUS 1 MW-70 m wind turbine manufactured by Siemens Company were selected as an efficient PV module and wind turbine for the proposed solar PV plant and wind farm project, respectively. The results showed that the large-scale wind farm is a more economical option than the solar PV plant because of the higher values of NPV and ALCS as well as the lower values of EP and LCOE.

References

Abdeladim K, Bouchakour S, Arab AH, Amrouche SO, Yassaa N (2018) Promotion of renewable energy in some MENA region countries. IOP Conf Ser Earth Environ Sci 154:012003. https://doi.org/10.1088/1755-1315/154/1/012003

Adaramola MS (2014) Viability of grid-connected solar PV energy system in Jos, Nigeria. Int J Electr Power Energy Syst 61:64–69. https://doi.org/10.1016/j.ijepes.2014.03.015

Ahmed AS (2019) Analysis the economics of sustainable electricity by wind and its future perspective. J Clean Prod 224:729–738. https://doi.org/10.1016/j.jclepro.2019.03.246

Al Zohbi GA, Hendrick P, Bouillard P (2015) Wind characteristics and wind energy potential analysis in five sites in Lebanon. Int J Hydrogen Energy 40(44):15311–15319. https://doi.org/10.1016/j.ijhydene.2015.04.115

Al Zohbi GA, Hendrick P, Renier C, Bouillard P (2016) The contribution of wind-hydro pumped storage systems in meeting Lebanon's electricity demand. Int J Hydrogen Energy 41(17):6996–7004. https://doi.org/10.1016/j.ijhydene.2016.01.028

Alayat M, Kassem Y, Çamur H (2018) Assessment of wind energy potential as a power generation source: a case study of eight selected locations in Northern Cyprus. Energies 11(10):2697. https://doi.org/10.3390/en11102697

Alsaad M (2013) Wind energy potential in selected areas in Jordan. Energy Convers Manag 65:704–708. https://doi.org/10.1016/j.enconman.2011.12.037

Chadee XT, Clarke RM (2018) Wind resources and the levelized cost of wind generated electricity in the Caribbean islands of Trinidad

and Tobago. Renew Sustain Energy Rev 81:2526–2540. https://doi.org/10.1016/j.rser.2017.06.059
Chang B, Starcher K (2019) Evaluation of wind and solar energy investments in Texas. Renew Energy 132:1348–1359. https://doi.org/10.1016/j.renene.2018.09.037
Chedid R, Chaaban F, Salameh S (2001) Policy analysis of greenhouse gas emissions: the case of the Lebanese electricity sector. Energy Convers Manag 42(3):373–392. https://doi.org/10.1016/S0196-8904(00)00060-1
Dabar OA, Awaleh MO, Kirk-Davidoff D, Olauson J, Söder L, Awaleh SI (2019) Wind resource assessment and economic analysis for electricity generation in three locations of the Republic of Djibouti. Energy 185:884–894. https://doi.org/10.1016/j.energy.2019.07.107
Danook SH, Jassim KJ, Hussein AM (2019) The impact of humidity on performance of wind turbine. Case Stud Therm Eng 14:100456. https://doi.org/10.1016/j.csite.2019.100456
Elkhoury M, Nakad Z, Shatila S (2010) The assessment of wind power for electricity generation in Lebanon. Energy Sources Part A Recovery Util Environ Effects 32(13):1236–1247. https://doi.org/10.1080/15567030802706754
Fazelpour F, Markaria E, Soltani N (2017) Wind energy potential and economic assessment of four locations in Sistan and Balouchestan province in Iran. Renew Energy 109:646–667. https://doi.org/10.1016/j.renene.2017.03.072
Gökçekuş H, Kassem Y, Al Hassan M (2019) Evaluation of wind potential at eight selected locations in Northern Lebanon using open source data. Int J Appl Eng Res 14(11):2789–2794
Guerrero-Villar F, Dorado-Vicente R, Fike M, Torres-Jiménez E (2019) Influence of ambient conditions on wind speed measurement: impact on the annual energy production assessment. Energy Convers Manag 195:1111–1123. https://doi.org/10.1016/j.enconman.2019.05.067
Gul M, Tai N, Huang W, Nadeem M, Yu M (2019) Assessment of wind power potential and economic analysis at hyderabad in Pakistan: powering to local communities using wind power. Sustainability 11(5):1391. https://doi.org/10.3390/su11051391
Ibarra-Berastegi G, Ulazia A, Saénz J, González-Rojí SJ (2019) Evaluation of Lebanon's offshore-wind-energy potential. J Mar Sci Eng 7(10):361. https://doi.org/10.3390/jmse7100361
Irwanto M, Gomesh N, Mamat M, Yusoff Y (2014) Assessment of wind power generation potential in Perlis, Malaysia. Renew Sustain Energy Rev 38:296–308. https://doi.org/10.1016/j.rser.2014.05.075
Kassem Y (2018) Computational study on vertical axis wind turbine car: static study. Model Earth Syst Enviro 4(3):1041–1057. https://doi.org/10.1007/s40808-018-0461-x
Kassem Y, Camur H, Abughinda SA, Sefik A (2019a) Wind energy potential assessment in selected regions in Northern Cyprus based on Weibull distribution function. J Eng Appl Sci 15(1):128–140
Kassem Y, Gökçekuş H, Çamur H (2019b) Artificial neural networks for predicting the electrical power of a new configuration of savonius rotor. Advances in intelligent systems and computing 10th international conference on theory and application of soft computing, computing with words and perceptions. ICSCCW. https://doi.org/10.1007/978-3-030-35249-3_116
Kassem Y, Gökçekuş H, Zeitoun M (2019c) Modeling of techno-economic assessment on wind energy potential at three selected coastal regions in Lebanon. Model Earth Syst 5(3):1037–1049. https://doi.org/10.1007/s40808-019-00589-9
Kassem Y, Gökçekuş H, Mizran MM, Alsayas SM (2019d) Evaluation of the wind energy potential in Lebanon's coastal regions using Weibull distribution function. Int J Eng Res Technol 12(6):784–792
Kassem Y, Zoubi R, Gökçekuş H (2019e) The possibility of generating electricity using small-scale wind turbines and solar photovoltaic systems for households in Northern Cyprus: a comparative study. Environments 6(4):47. https://doi.org/10.3390/environments6040047
Kassem Y, Çamur H, Alhuoti SMA (2020) Solar energy technology for Northern Cyprus: assessment, statistical analysis, and feasibility study. Energies 13(4):940. https://doi.org/10.3390/en13040940
Keyhani A, Ghasemi-Varnamkhasti M, Khanali M, Abbaszadeh R (2010) An assessment of wind energy potential as a power generation source in the capital of Iran, Tehran. Energy 35(1):188–201. https://doi.org/10.1016/j.energy.2009.09.009
Khan MA, Çamur H, Kassem Y (2018) Modeling predictive assessment of wind energy potential as a power generation sources at some selected locations in Pakistan. Model Earth Syst Environ 5(2):555–569. https://doi.org/10.1007/s40808-018-0546-6
Laqui W, Zubieta R, Rau P, Mejía A, Lavado W, Ingol E (2019) Can artificial neural networks estimate potential evapotranspiration in Peruvian highlands? Model Earth Syst Environ 5(4):1911–1924. https://doi.org/10.1007/s40808-019-00647-2
Mohammadi K, Alavi O, Mcgowan JG (2017) Use of Birnbaum-Saunders distribution for estimating wind speed and wind power probability distributions: a review. Energy Convers Manag 143:109–122. https://doi.org/10.1016/j.enconman.2017.03.083
Nakad Z, Elkhoury M, Arnaout JP, Shatila S (2012) A feasibility study on establishing wind farms in Lebanon. Energy Sources Part B 7(4):366–375. https://doi.org/10.1080/15567241003645531
Olaofe ZO, Folly KA (2013) Wind energy analysis based on turbine and developed site power curves: a case-study of Darling City. Renew Energy 53:306–318. https://doi.org/10.1016/j.renene.2012.11.003
Osinowo AA, Okogbue EC, Eresanya EO, Akande OS (2017) Evaluation of wind potential and its trends in the mid-Atlantic. Modeling Earth Systems and Environment 3(4):1199–1213. https://doi.org/10.1007/s40808-017-0399-4
Owolabi AB, Nsafon BEK, Roh JW, Suh D, Huh JS (2019) Validating the techno-economic and environmental sustainability of solar PV technology in Nigeria using RETScreen Experts to assess its viability. Sustain Energy Technol Assess 36:100542. https://doi.org/10.1016/j.seta.2019.100542
Owusu PA, Asumadu-Sarkodie S (2016) A review of renewable energy sources, sustainability issues and climate change mitigation. Cogent Eng 3:1. https://doi.org/10.1080/23311916.2016.1167990
Parikh V, Desai C, Joshi D, Nagababu G (2019) Estimation of electricity generation potential by solar radiation on Sardar Sarovar dam. Energy Proced 158:167–172. https://doi.org/10.1016/j.egypro.2019.01.065
Pishgar-Komleh S, Keyhani A, Sefeedpari P (2015) Wind speed and power density analysis based on Weibull and Rayleigh distributions (a case study: Firouzkooh county of Iran). Renew Sustain Energy Rev 42:313–322. https://doi.org/10.1016/j.rser.2014.10.028
Prasad AA, Taylor RA, Kay M (2017) Assessment of solar and wind resource synergy in Australia. Appl Energy 190:354–367. https://doi.org/10.1016/j.apenergy.2016.12.135
Prăvălie R, Patriche C, Bandoc G (2019) Spatial assessment of solar energy potential at global scale: a geographical approach. J Clean Prod 209:692–721. https://doi.org/10.1016/j.jclepro.2018.10.239
Rafique M, Rehman S, Alam M, Alhems L (2018) Feasibility of a 100 MW installed capacity wind farm for different climatic conditions. Energies 11(8):2147. https://doi.org/10.3390/en11082147
Rehman S, Ahmed M, Mohamed MH, Al-Sulaiman FA (2017) Feasibility study of the grid connected 10 MW installed capacity PV power plants in Saudi Arabia. Renew Sustain Energy Rev 80:319–329. https://doi.org/10.1016/j.rser.2017.05.218
Shu Z, Li Q, Chan P (2015) Statistical analysis of wind characteristics and wind energy potential in Hong Kong. Energy Convers Manag 101:644–657. https://doi.org/10.1016/j.enconman.2015.05.070

Tannous S, Manneh R, Harajli H, Zakhem HE (2018) Comparative cradle-to-grave life cycle assessment of traditional grid-connected and solar stand-alone street light systems: a case study for rural areas in Lebanon. J Clean Prod 186:963–977. https://doi.org/10.1016/j.jclepro.2018.03.155

Ulazia A, Sáenz J, Ibarra-Berastegi G, González-Rojí SJ, Carreno-Madinabeitia S (2019) Global estimations of wind energy potential considering seasonal air density changes. Energy 187:115938. https://doi.org/10.1016/j.energy.2019.115938

Yue W, Xue Y, Liu Y (2017) High humidity aerodynamic effects study on offshore wind turbine airfoil/blade performance through CFD analysis. Int J Rotat Mach 2017:1–15. https://doi.org/10.1155/2017/7570519

Zendehboudi A, Baseer M, Saidur R (2018) Application of support vector machine models for forecasting solar and wind energy resources: a review. J Clean Prod 199:272–285. https://doi.org/10.1016/j.jclepro.2018.07.164

ZhouWx YWU, Liu G (2011) Assessment of onshore wind energy resource and wind-generated electricity potential in Jiangsu, China. Energy Proced 5:418–422. https://doi.org/10.1016/j.egypro.2011.03.072